AN INVESTIGATION OF THE REQUIREMENTS OF A TURBO PROP CONTROL SYSTEM THROUGH USE OF THE ELECTRONIC DIFFERENTIAL ANALYZER

BY

ARTHUR MCDOWELL CARTER, JR.

AND

DANIEL WILLIAM WILDFONG

AN INVESTIGATION OF THE REQUIREMENTS OF A TURBO PROP CONTROL SYSTEM THROUGH USE OF THE ELECTRONIC DIFFERENTIAL ANALYZER

A
THESIS
SUBMITTED TO
THE AERONAUTICAL ENGINEERING DEPARTMENT
FOR
THE DEGREE OF MASTER OF SCIENCE IN ENGINEERING
BY
ARTHUR MCDOWELL CARTER, JR.
AND
DANIEL WILLIAM WILDFONG

UNIVERSITY OF MICHIGAN
ANN ARBOR, MICHIGAN

JUNE 1950

TABLE OF CONTENTS

SECTION I

SUMMARY

The adaptability of the differential analyzer in solving the turbo prop control system problem was investigated in this study, and some of the more fundamental results which are obtainable by this method of approach are herein presented.

The basic control assumption used in this investigation was that rotational speed be governed by blade angle. Temperature was neglected, and fuel flow was considered as a step input resulting in an instantaneous increase in torque.

It was found that adequate response at a given operating condition could be obtained by assuming blade angle a function of offspeed and integral of offspeed. At other operating conditions, however, there was a wide variation in response. This variation in response was reduced by requiring blade angle to vary, in addition to the previous assumptions, as the derivative of the offspeed.

It was concluded that the differential analyzer has definite merit for application to this control problem, both for analysis and for possible actual installation as the controlling unit.

This investigation is but an infant's step toward a very adult problem. Additional and amplifying procedures and methods of approach,

not possible of accomplishment due mainly to lack of time, are hereinafter presented.

SECTION II

INTRODUCTION

Analysis of the characteristics of power plants available for the propulsion of aircraft clearly indicates the place for the turbo-prop power plant. The highly developed reciprocating engine has proven itself in the speed range up to 400 MPH. The turbo-jet would seem to be the answer where very high speed, 550 MPH and above, is specified; but this high speed is accompanied with the disadvantage of short range due to the high fuel consumption of the turbo-jet engine. The turbo-prop power plant fills the speed gap between 400 and 550 MPH and in addition, excellent range can be obtained. With the development of the supersonic propeller, the speed of turbo-prop powered aircraft might well reach that of turbo-jet powered craft. Thus the need for the turbo-prop power plant is apparent, both for commercial and military operations.

The turbo-prop power plant consists essentially of a gas turbine driving a propeller through reduction gearing. The control problem for such a system is inherently complex because of the number of variables which enter into the problem and the interrelation of the variables. The five primary variables are Engine Speed, Torque,

Temperature, Fuel Flow, and Propeller Blade Angle. In addition, maximum engine efficiency is attained at nearly maximum allowable turbine speed and temperature, thereby requiring operation in a regime having narrow control limitations on certain of the variables.

The ultimate requirement for a turbo-prop control system is that the pilot be able to select a desired value of power, without exceeding any of the design limitations of the power plant components. A great amount of research is at present being conducted in an attempt to obtain such a control system.

In References 1, 2 and 3, a general discussion of the control requirements for turbo-prop power plants is given. In Ref. 4, the adaptability of the electronic differential analyzer to the analysis of the requirements of the control system is discussed. In Ref. 5, the utility of the electronic differential analyzer for obtaining solutions to engineering problems is considered, and a complete description of the type analyzer used in this investigation is given.

It was the purpose of this investigation, in addition to giving the authors practice in the use of the electronic analyzer, to carry out a study of the basic requirements of the control system for a turbo-prop power plant. Since the purpose did not include the design of such a system, a fundamental approach has been attempted throughout. The method followed was to start with an initial, simplified equation representing the basic characteristics of the turbo-prop power plant, and to add to the initial system, as time allowed, certain functions which would improve the response characteristics of the control system.

It is regretted that due to time limitations, a more complete investigation could not be made.

The authors wish to express their appreciation to Doctor L. L. Rauch, Department of Aeronautical Engineering, University of Michigan, for his assistance and guidance throughout this investigation; and also to Professor J. W. Luecht, Department of Aeronautical Engineering, University of Michigan, for his assistance in obtaining the engine and propeller data used, and in the reduction of this data to a usable form.

SECTION III A

DEVELOPMENT OF BASIC EQUATIONS

Definition of symbols and terminology:

Subscripts:

a - aerodynamic

c - compressor

e - engine

p - propeller

t - turbine

w_f - fuel flow

Superscripts:

* - steady state

Symbols:

$C_{e_{\Omega_E}} = (\partial Q_E/\partial \Omega_E)_{W_f}$

$C_{e_{w_f}} = (\partial O_E/\partial W_f)_{\Omega_E}$

$C_{p_\beta} = (\partial Q_a/i/\partial \beta)_{\Omega_E}$

$C_{p_{\Omega_E}} = (\partial Q_a/i/\partial \Omega_E)_\beta$

I_e - Moment of inertia of the engine

I_p/i^2 - Moment of inertia of the propeller referred to the engine

Q_a - Instantaneous aerodynamic torque absorbed by the propeller

Q_e - Instantaneous net engine torque (equals $Q_t - Q_c$)

Q_{pe} - Instantaneous engine torque delivered to the reduction gears

Q_{pp} - Instantaneous torque to propeller from reduction gears

$(Q_e - Q_{pe})$ - Instantaneous torque available for acceleration of the engine

$(Q_{pp} - Q_a)$ - Instantaneous torque available for acceleration of the propeller

$q = Q_{pe} - Q^*_{pe}$ - Difference between instantaneous and steady state torque to reduction gears

$i = \Omega_E / \Omega_P$ - Reduction gear ratio

Ω - Rotation speed

β - Blade angle

θ - New variable introduced for ease of mathematical treatment

Relations:

Transient	Steady State
$Q_p = Q_{pp}/i$	$Q^*_{pe} = Q^*_{pp}/i$
$Q_e = Q_t - Q_c$	$Q^*_e = Q^*_t - Q^*_c$
$Q_e - Q_{pe} = I_e \, (d\Omega_E/dt)$	$Q^*_e = Q^*_{pe}$
$Q_{pp} - Q_a = I_p \, (d\Omega_P/dt)$	$Q^*_a = Q^*_{pp}$

$$\text{Also; } \left.\begin{aligned} d\Omega_E/dt &= d(\Omega_E - \Omega^*_E)/dt \\ d\Omega_P/dt &= d(\Omega_P - \Omega^*_P)/dt \end{aligned}\right\} \text{since steady state derivative is zero}$$

Development of engine equation:

Note: Constant density ratio, temperature ratio, and flight velocity assumed here and also in the development of the propeller equation.

From above:

$$Q_e - Q_{pe} = I_e \, d(\Omega_E - \Omega_E^*)/dt ,$$

where

$$Q_e = Q_e(W_f, \Omega_E) = Q_e(W_f^* + dw_f, \Omega_E^* + d\Omega_E),$$

$$Q_e = Q_e^* + (\partial Q_e/\partial w_f)_{\Omega_E} \, dw_f + (\partial Q_e/\partial \Omega_E)_{w_f} \, d\Omega_E,$$

$$O_e = Q_e^* + C_{ew_f} \, dw_f + C_{e\Omega_E} \, d\Omega_E .$$

But

$$Q_{pe} = Q_{pe}^* + q, \text{ and } Q_e^* = Q_{pe}^* .$$

Therefore, the engine equation is:

$$I_e \, d(\Omega_E - \Omega_E^*)/dt = C_{ew_f} \, dw_f + C_{e\Omega_E} \, d\Omega_E - q. \quad (1)$$

Development of propeller equation:

From above:

$$Q_{pp} - Q_a = I_p \, d(\Omega_p - \Omega_p^*)/dt .$$

Therefore

$$Q_{pe} - Q_a/i = I_p/i \, d(\Omega_E - \Omega_E^*/i)/dt = I_p/i^2 \, d(\Omega_E - \Omega_E^*)/dt,$$

where, $Q_a = Q_a(\Omega_E, \beta) = Q_a(\Omega_E^* + d\Omega_E, \beta^* + d\beta)$,

$$Q_a = Q_a^* + (\partial Q_a/\partial \Omega_E)_\beta \, d\Omega_E + (\partial Q_a/\partial \beta)_{\Omega_E},$$

$$Q_a = Q_a^* + i\, C_{p\Omega_E}\, d\Omega_E + i\, C_{p\beta}\, d\beta,$$

$$Q_a/i = Q_a^*/i + C_{p\Omega_E}\, d\Omega_E + C_{p\beta}\, d\beta.$$

Therefore,

$$I_p/i^2 \, d(\Omega_E - \Omega_E^*)/dt = Q_{pe} - Q_a^*/i - C_{p\Omega_E}\, d\Omega_E - C_{p\beta}\, d\beta.$$

But,

$$Q_{pe} = Q_{pe}^* + q, \text{ and } Q_a^*/i = Q_{pe}^*.$$

Therefore the propeller equation is:

$$I_p/i^2 \, d(\Omega_E - \Omega_E^*)/dt = q - C_{p\Omega_E}\, d\Omega_E - C_{p\beta}\, d\beta. \quad (2)$$

Development of combined equation:

$$I_E \, d(\Omega_E - \Omega_E^*)/dt = C_{ew_f}\, dw_f + C_{e\Omega_E}\, d\Omega_E - q. \quad (1)$$

$$I_p/i^2 \, d(\Omega_E - \Omega_E^*)/dt = q - C_{p\Omega_E}\, d\Omega_E - C_{p\beta}\, d\beta. \quad (2)$$

Eliminating q and substituting differences for differentials:

$$(I_E + I_p/i^2)\, d(\Omega_E - \Omega_E^*)/dt + C_{p\beta}(\beta - \beta^*) + (C_{p\Omega_E} + C_{E\Omega_E})(\Omega_E - \Omega_E^*) = C_{ew_f}(w_f - w_f^*). \quad (3)$$

Equation (3) is the basic equation used in this investigation.

SECTION III B

DATA ON THE T. G. 100, TURBO-PROP ENGINE

For purposes of this investigation, operating data on the General Electric T. G. 100 turbo-prop engine, as presented in Ref. 6, was used exclusively since this was the only data available to the authors in an unrestricted form. The fact that the T. G. 100 is essentially a constant speed engine, does not reduce its value as representative of a turbo-prop engine, but does simplify the control problem to some extent. In a variable speed engine, a new engine speed accompanies each new power plant output called for, in order to operate at maximum system efficiency. This affects the control system problem in that this new engine speed would have to be called for, or scheduled.

For this investigation, a flight velocity of 300 MPH was assumed for Step I; and for Step II, velocities of 100, 300, and 500 MPH were assumed; all at a fuel flow rate of 1400 lbs/hr and at sea level. In order to evaluate the coefficients for the equation representing the power plant, the values of total shaft horsepower listed in Table I were obtained from Figure OA of Section 24, Ref. 6, reproduced in this report as Figure 2. The friction loss was obtained from Figure 23 of Section 23, Ref. 6, and subtracted from the total shaft

horsepower thus obtaining the Engine Shaft horsepower (SHP_e). This was then converted to engine torque (Q_e).

$$\left[Q_e, \text{ft. lbs.} = SHP_e \times \frac{33{,}000}{2\pi(\Omega_e, RPM)} \right]$$

. A plot of Engine Torque (Q_e) versus Engine Speed (Ω_e) with fuel flow rate (w_f) as parameter was then made for 100, 300 and 500 MPH flight velocities in Figures 3, 4 and 5 respectively. The slope of these curves gives the coefficient $C_{e_{\Omega_e}} = \left(\frac{\partial Q_e}{\partial \Omega_e}\right)_{w_f}$ for the operating condition (velocity, and engine power) chosen. The value of $C_{e_{\Omega_e}}$ for flight velocities of 100, 300 and 500 MPH at sea level and w_f of 1400 lbs/hr are given in Table III.

The polar moment of inertia of the rotating elements of the engine (turbine, compressor rotor, reduction gearing, and accessories) is given in Ref. 6 as $I_e = 4.008$ slug ft.^{2} .

SECTION III C

SELECTION OF PROPELLER

Definition of symbols:

C_p (Power Coefficient) = $\frac{P}{\rho n^3 D^5}$

ρ = mass density of air (slugs per cubic foot).

n = propeller rotational speed (revolutions per second).

D = propeller diameter (feet).

V = airspeed (feet per second).

β = blade angle (degrees) at 0.75 propeller radius.

Since there was no available information on the propeller intended for use with the T. G. 100 engine, it was necessary to select a suitable one. The best information available on propellers suitable for this type installation was found in Ref. 7. The theory as presented in Ref. 8 was utilized in conjunction with Ref. 7 to determine the most suitable propeller possible.

Ref. 7 contains information only on ten foot diameter propellers. Of the propellers considered, the one finally determined as capable of absorbing the engine power available was a six wide blade, dual rotating tractor propeller, the characteristics of which are given in Figure 16 of Ref. 7, reproduced as Figure 6 of this report. In order to check the suitability of this propeller, combinations of flight speed,

engine power, and engine RPM were selected at sea level, and $\frac{V}{nD}$ and C_p computed. Entering Figure 6 with these values of $\frac{V}{nD}$ and C_p, points indicating β and propeller efficiency were determined. Plotting a number of these points for speeds of 100, 300 and 500 MPH indicated that at 300 MPH the points were to the left of maximum efficiency, while for 500 MPH, the points were to the right. This phenomena was caused by too large a variation in $\frac{V}{nD}$ due to the fact that an initial basic premise was constant engine rotational velocity for steady-state operation. This loss of propeller efficiency was disregarded because, for the purpose of this analysis, only adequate power absorption of the propeller is important, not power output. Since this situation does exist, however, it is implied that even though an engine of itself gives maximum economy at full rated RPM, a simultaneous schedule of fuel flow and RPM instead of fuel flow only, is necessary to compensate for the loss in efficiency of the propeller.

Having decided that the propeller was acceptable, the arguments for Table II were obtained from Figure 6 by entering this Figure with $\frac{V}{nD}$ and reading off C_p for various β. From this table, Figures 7 through Figure 12 were constructed for the three speeds selected for analysis. These curves are plots of $\frac{Q_a}{i}$ vs β with Ω_E as parameter and $\frac{Q_a}{i}$ vs Ω_E with β as parameter. The purpose of these curves is simply to enable determination of C_{p_β} and $C_{p_{\Omega_E}}$ for each operating condition analyzed so that these coefficients might be inserted in the general differential equation representing the system. C_{p_β} and $C_{p_{\Omega_E}}$ are slopes at the particular operating condition, being equal to $\left(\partial Q_a/i/\partial\beta\right)_{\Omega_E}$ and $\left(\partial Q_a/i/\partial\Omega_E\right)_\beta$, respectively. The coefficients for flight speeds of 100, 300, and 500 MPH at sea level and w_f of 1400 lbs/hr are tabulated in Table III.

One other quantity needed is the moment of inertia of the propeller. Whether of the solid aluminum alloy or hollow steel type, the result was essentially the same. One method of approach is illustrated in Ref. 8, and is applicable to aluminum alloy blades. The estimated I_p using the method of Ref. 8 was 70.2 slug feet^2.

SECTION III

THE ELECTRONIC DIFFERENTIAL ANALYZER

A complete, detailed description of the electronic differential analyzer used in this investigation is given in Ref. 5, and therefore will not be repeated herein. In general the analyzer consists of plug-in feedback amplifier units which by simple external changes in connection can be used for integration, differentiation, multiplication and division by constants, summation and sign changing.

For recording data, the desired outputs from the analyzer were fed into Brush, Model BL-913 direct current amplifiers (modified), the output of which was fed into a two-channel Brush, Model BL-202, magnetic type, recording oscillograph.

A picture of a typical analyzer set-up is given in Figure 13.

SECTION III E

PROCEDURE

The basic equation representing the power plant is equation (3) (see Section III A above).

$$\left[I_e + I_p/i^2\right](\dot{\Omega}_E - \Omega_E^*) + C_{p\beta}(\beta - \beta^*) + \left[C_{p\Omega_E} - C_{e\Omega_E}\right](\Omega_E - \Omega_E^*)$$

$$= C_{e_{w_f}}(w_f - w_f^*) \; . \qquad (3)$$

For purposes of analysis, a new variable is introduced, i.e.;

$$\theta = \int(\Omega_E - \Omega_E^*)\,dt,$$

$$\dot{\theta} = (\Omega_E - \Omega_E^*),$$

$$\ddot{\theta} = (\dot{\Omega}_E - \Omega_E).$$

Substituting Θ in equation (3), the basic equation becomes:

$$\left[I_e + I_p/i^2\right]\ddot{\theta} + C_{p\beta}(\beta - \beta^*) + \left[C_{p\Omega_E} - C_{e\Omega_E}\right]\dot{\theta}$$

$$= C_{e_{w_f}}(w_f - w_f^*). \qquad (4)$$

If it is now assumed that the propeller pitch control changes propeller pitch at a rate proportional to the engine offspeed, then

$$d\beta/dt = k_1(\Omega_E - \Omega_E^*),$$

$$\beta = \beta^* + k_1\int_0^t(\Omega_E - \Omega_E)\,dt = \beta^* + k_i\,\theta,$$

$$\beta - \beta^* = k_1\int_0^t(\Omega_E - \Omega_E^*)\,dt = k_1\,\theta \; , \qquad (5)$$

where k_1 is the governor proportionality constant. This type of control on propeller pitch will be termed "integral control on β".

Substituting this value of $(\beta - \beta^*)$ in equation (4), the following second order differential equation is obtained:

$$\left[I_E + I_P/i^2\right]\ddot{\theta} + \left[C_{P\Omega_E} - C_{e\Omega_E}\right]\dot{\theta} + \left[C_{P\beta}\,k_1\right]\theta$$
$$= C_{e_{w_f}}\left(w_f - w_f^*\right). \qquad (6)$$

Analysis of the engine and propeller curves, Figure 3 through Figure 12, indicates that the coefficients of equation (6) remain practically constant over a reasonable range of operation, the inertia term naturally remaining constant.

If the coefficients are considered as constant, equation (6) is comparable to the standard single degree of freedom vibratory equation

$$a_2\ddot{\theta} + a_1\dot{\theta} + a_0\theta = f(t),$$

where $a_2 = \left[I_e + I_P/i^2\right]$ is the inertia or mass term,

$a_1 = \left[C_{P\Omega_E} - C_{e\Omega_E}\right]$ is the damping term,

and $a_0 = \left[C_{P\beta}\,k_1\right]$ is the spring constant term.

The known procedure for the analysis of this type equation can now be followed.

(A) Step 1.

As indicated in Ref. 3, the natural damping term $(C_{P\Omega_E} - C_{e\Omega_E})$ of the system is insufficient for adequate response.

The natural damping was therefore augmented by requiring the prop pitch control to change pitch at a rate proportional to the

derivative of engine offspeed, in addition to the engine offspeed.

Then

$$d\beta/dt = k_1(\Omega_E - \Omega_E^*) + k_2(\dot{\Omega}_E - \dot{\Omega}_E^*),$$

$$\beta - \beta^* = k_1\int_0^t (\Omega_E - \Omega_E^*)\,dt + k_2(\Omega_E - \Omega_E^*),$$

$$\beta - \beta^* = k_1\theta + k_2\dot{\theta}. \qquad (7)$$

The basic equation after substitution then becomes

$$\left[I_E + I_P/i^2\right]\ddot{\theta} + \left[C_{p\Omega_E} - C_{e\Omega_E} + C_{p\beta}k_2\right]\dot{\theta} + C_{p\beta}k_1\theta$$
$$= C_{ew_f}(w_f - w_f^*). \qquad (8)$$

For purposes of analysis, it is convenient to consider the right side of equation (8) as a step input of engine torque (q_e) resulting from a step input of fuel flow rate ($w_f - w_f^*$); and then to determine the response characteristics of the system due to such a step input. It is considered that this is a conservative approach, since the effect of an actual change in fuel flow rate, involving necessarily a finite rate of change, would represent a less stringent condition.

The basic equation, equation (8), can now be expressed as

$$\left[I_e + I_p/i^2\right]\ddot{\theta} + \left[C_{p\Omega_E} - C_{e\Omega_E} + C_{p\beta}k_2\right]\dot{\theta} + C_{p\beta}k_1\theta$$
$$= q_{w_f},$$

where $a_2 = \left[I_e + I_p/i^2\right]$ is the inertia term,

$a_1 = \left[C_{p\Omega_E} - C_{e\Omega_E} + C_{p\beta}k_2\right]$ is the augmented damping term,

$a_0 = \left[\ C_{p\beta}k_1\ \right]$ is the spring constant term.

Various values of damping ratio ($\zeta = a_1/2\sqrt{a_0 a_2}$) were next assumed; and for each value of damping ratio, various values of the natural undamped frequency $(\omega_n = \sqrt{a_0/a_2})$ of the system were assumed. Since the value of the inertia term (a_2) is known and remains constant, the value of the damping term (a_1) and the spring constant term (a_0) could be determined for each combination of ζ and ω_n chosen: i.e.

$$a_2 = I_e + I_p/i^2 = 4.008 + .542 = 4.55,$$

$$a_0 = a_2 \omega_n^2 = 4.55\, \omega_n^2,$$

$$a_1 = 2\zeta\sqrt{a_0 a_2}.$$

For this part of the investigation, a cruising operating condition at sea level was assumed, with a flight velocity (V_0) of 300 MPH and fuel flow rate (w_f) of 1400 lbs/hr. For this condition, the values of $C_{p\Omega_E}$, $C_{e\Omega_E}$, and $C_{p\beta}$ had previously been determined and the values listed in Table III. It was then possible to evaluate the proportionality constants k_1 and k_2, since

$$k_1 = a_0/C_{p\beta},$$

$$k_2 = \frac{a_1 - C_{p\Omega_E} - C_{e\Omega_E}}{C_{p\beta}}.$$

For completeness of information, the value of the natural damped frequency (ω) of the system for each combination of ζ and ω_n was determined by $\omega = \omega_n\sqrt{1-\zeta^2}$.

The values of a_0, a_1, k_1, and k_2 for the combinations of ζ and ω_n chosen are given in Table IV. The reciprocals of the coefficients are also given since they are used in the analyzer set up.

All coefficients having been determined, the differential analyzer was set up. The diagram of the analyzer circuit is given in Figure 18. Amplifiers A_1 through A_6 are used to solve the basic equation (equation (9)); while amplifiers A_7 and A_8 were added to solve the engine equation (equation (1)) for q, in order to record this variable. The step input of torque due to change in fuel flow rate (q_{w_f}) was applied as a battery voltage across the inputs to amplifiers A_2 and A_7 when the switch S_1 was closed. An example of the record of a typical step input (q_{w_f}) on the Brush recorder is given in Figure 19.

In order to stay within the voltage limitations of the amplifiers (approximately 0.5 volts to 100 volts), it was necessary to change certain input and feedback amplifier resistances by factors of ten. This resulted in some of the variables recorded being different from the actual values by a multiplication factor, the factor being indicated in Figure 18. A correction for this factor was made when the recorded data was reduced.

The outputs of amplifiers A_3, ($\Omega_E - \Omega_E^*$); A_4 (θ); A_6 ($\beta - \beta^*$); and A_8, (q) were recorded.

For each combination of ζ and ω_n, the proper coefficients, as given in Table IV, were inserted in the analyzer in the proper position, as indicated in Figure 18.

A step input, q_{w_f}, was then applied for each combination and Brush oscillograph traces taken of the response of the variables ($\Omega_E - \Omega_E^*$), (q), ($\beta - \beta^*$), and (θ). The recorded oscillograph traces are shown in Figure 14 through Figure 17, respectively.

(B) Step 2.

As will be seen from the results of this step, the response of the control system varies over a wide range with changes in flight velocity if the type of propeller pitch control described in Step 1 is employed. If for instance, the proportionality constants k_1 and k_2 are chosen to give proper response at 300 MPH, then these same constants coupled with the coefficients corresponding to a different speed cause less damping at lower flight velocities and more damping at higher velocities. This change in response with change in speed is illustrated by the 0% D.C. curve of Figure 20. (% D.C. refers to the percent derivative control used and is defined later on in this section). It would be desirable if the control system could provide approximately constant optimum response over the complete range of flight velocity. To approach this result we will therefore require the propeller pitch control to change pitch at a rate proportional to the second derivative of the engine offspeed in addition to the requirements of Step 1. Thus

$$d\beta/dt = k_1(\Omega_E - \Omega_E^*) + k_2(\dot{\Omega}_E - \Omega_E^*) + k_3(\ddot{\Omega}_E - \Omega_E),$$

$$\beta - \beta^* = k_1\int_0^t(\Omega_E - \Omega_E^*)dt + k_2(\Omega_E - \Omega_E^*) + k_3(\dot{\Omega}_E - \Omega_E^*),$$

$$\beta - \beta^* = k_1\,\theta + k_2\,\dot{\theta} + k_3\,\ddot{\theta},$$

where k_3 is another propeller pitch control proportionality constant. This added term can be called "anticipatory" or "derivative control on β".

Again substituting in equation (3), the basic equation for Step 2 becomes

$$\left[I_e + I_p/i^2 + C_{p\beta} k_3\right]\ddot{\theta} + \left[C_{p\lambda_E} + C_{e\lambda_E} + C_{p\beta} k_2\right]\dot{\theta} + C_{p\beta} k_1 \theta = q_{w_f},$$

where $a_2 = \left[I_e + I_p/i^2 + C_{p\beta} k_3\right]$ is the inertia term,

$a_1 = \left[C_{p\lambda_E} + C_{e\lambda_E} + C_{p\beta} k_2\right]$ is the damping term,

$a_0 = \left[C_{p\beta} k_1\right]$ is the spring constant term.

It is seen that the addition of derivative control on β can be considered as an addition to the inertia term (a_2) of equation (10), thus giving a new "effective" inertia. The basic equation remains in the form of the standard vibratory equation and can be analyzed in a manner similar to that used in Step 1.

An undamped natural frequency (ω_n) of 5 rad/sec was now arbitrarily chosen as representative of this type power plant at an operating condition of 300 MPH, and a damping ratio (ζ) of 0.6 was chosen as an optimum overall value at this speed. Since the derivative control on β can be considered to change the inertia term (a_2) of equation (10), the procedure followed was to increase the value of the inertia term by convenient percentages, i.e. 100%, 200%, and 300%. This percent increase was termed percent derivative control, and is abbreviated hereafter as "% D.C."

In order to cover the complete range of flight velocities, three representative operating conditions were chosen, i.e. low velocity of 100 MPH, cruising velocity of 300 MPH, and high velocity of 500 MPH;

all at sea level and a fuel flow rate of 1400 lbs/hr. The determination of the values of the coefficients $C_{p\beta}$, $C_{p\Omega_E}$, and $C_{e\Omega_E}$ for these operating conditions has already been described, and the values are given in Table III.

By maintaining $\zeta = .6$ and $\omega_n = 5$ for all values of % D. C. for the 300 MPH operating condition, it was possible to determine the values of k_1, k_2, k_3, and a_2, a_1, a_0 for each case.

$$k_3 = \frac{[\% DC][I_e + I_p/i^2]}{C_{p\beta}}$$

$$a_2 = [1 + \% DC][I_e + I_p/i^2]$$

$$a_0 = a_2 \omega_n^2$$

$$k_1 = a_0/C_{p\beta}$$

$$a_1 = 2\zeta\sqrt{a_0 a_2} = [C_{p\Omega_E} - C_{e\Omega_E} + C_{p\beta} k_2]$$

$$k_2 = \frac{a_1 - C_{p\Omega_E} + C_{e\Omega_E}}{C_{p\beta}}$$

The calculated values of a_0, a_1, a_2, k_1, k_2, and k_3 for flight velocity of 300 MPH are given in Table V.

The values of k_1, k_2, and k_3 thus determined for each % D.C. for the 300 MPH operating condition were used for the corresponding % D.C. at the other flight velocities chosen. It was then possible to calculate the coefficients (a_0, a_1, a_2) of the basic equation at each % D.C. and airspeed, and therefore the ζ and ω_n.

$$a_0 = C_{p\beta} k_1$$

$$a_1 = C_{p\Omega_E} - C_{e\Omega_E} + C_{p\beta} k_2$$

$$a_2 = \left[1 + \% DC\right]\left[I_e + I_p/i^2\right]$$

$$\zeta = a_1 / 2\sqrt{a_0 a_2}$$

$$\omega_n = \sqrt{a_0/a_2}$$

The values determined for these two operating conditions are also given in Table V.

In Figure 20, a plot was made of ζ VS flight velocity (V_o) to show the theoretical effect of derivative control on the damping ratio.

The coefficients of the basic equation having been determined for all combinations of operating conditions and % D.C. chosen, the response of the system to a step input of torque (q_{wf}) was obtained using the analyzer in the same manner as described for Step 1, the same variables being recorded. The modified analyzer circuit diagram is given in Figure 18. The recorded oscillograph traces are shown in Figure 21 through Figure 24.

SECTION IV

RESULTS AND DISCUSSION

From the oscillograph of the four variables recorded, the maximum and steady state deviations in millimeters, slope in the case of β , and frequency and time to damp were obtained. These measurements in millimeters were translated into voltages by applying the calibration data and attenuator settings on the recorders, and also the multiplication factors made necessary by the voltage limitations of the analyzer amplifiers. These voltage magnitudes were then equal quantitatively to the value of the variable measured. The values of frequency and time to damp were difficult to obtain from the traces and therefore the absolute values given can be considered only approximate. Values of frequency not listed in the tables were impossible to measure from the traces. An example of the method used in the reduction of data is given in Section VII, Sample Calculations.

Step 1. Results

Step 1 was based on an original steady state torque of about 65% power. The step input of torque was 63.5 ft. lbs. or equivalent to roughly a 10% change in power based on the original steady state power. This corresponds to about a 6.5% change based on maximum power. Since

the coefficients of the differential equation for the system change only slightly with change in output of the engine, the equation can be assumed linear for all values of torque at one airspeed without too much error. For instance, if a jump from 65% to 100% torque were desirable, the results tabulated could be multiplied by 100-65/6.5=5.4 to give fairly good approximations of response.

In this step, it was assumed that β was a function of the integral of the offspeed and the offspeed. The traces taken are presented in Figure 14 through Figure 17, and are arranged to show the effect on response of changes in ζ and ω_n. Only relative and not quantitative comparisons of maximum and steady state values of $\Delta\Omega_E$ and θ shown on the traces may be made, due to the necessity of having different attenuation and calibration values set on the recorders. This was necessary in order to get traces of reasonable size. The reduced data is given in Table IV, and Figure 25 was drawn from the tabulated values.

Figure 25 shows the effect on maximum response values of q, Ω_E, β and $\frac{d\beta}{dt}$ of varying damping ratio (ζ) and natural undamped frequency (ω_n). It is seen that increasing ω_n results in lower maximum values of torque and engine offspeed, and higher maximum values of β and $\frac{d\beta}{dt}$. Increasing ζ, in general, decreases the maximum values of the variables plotted except for $\frac{d\beta}{dt}$ in which case the reverse is true.

In an actual control system, there would naturally be limits on the maximum allowable or obtainable $\frac{d\beta}{dt}$ and $\frac{d^2\beta}{dt^2}$. These limitations would partially define the design problem which could be solved by selecting proportionality constants (k_1 and k_2) to obtain the necessary ζ and ω_n for adequate response.

$\frac{d^2\beta}{dt^2}$ was not considered previously in this investigation due to the inability of measuring this quantity in all cases from the β traces. Several approximate values were obtained from the $\zeta = .3$ traces;

$$\left(\frac{d^2\beta}{dt^2}\right)_{\omega_n=2} = 1^\circ/sec^2 ,$$

$$\left(\frac{d^2\beta}{dt^2}\right)_{\omega_n=5} = 19.5^\circ/sec^2 ,$$

$$\left(\frac{d^2\beta}{dt^2}\right)_{\omega_n=10} = 150^\circ/sec^2 .$$

These average values were obtained from high speed traces (not included) by dividing $\left(\frac{d\beta}{dt}\right)_{MAX}$ by the time interval necessary to reach $\left(\frac{d\beta}{dt}\right)_{MAX}$. All values of $\frac{d^2\beta}{dt^2}$ could have been obtained in this fashion using the differential analyzer by merely changing the time base of the system or by setting up the system to record this variable.

It is understood that a typical system now in use would at least be capable of a $\frac{d\beta}{dt}$ of 10°/sec. in .03 sec. and therefore a $\frac{d^2\beta}{dt^2}$ of $333^\circ/sec^2$. Such values, once determined from the propeller governor characteristics, could be set on the differential analyzer.

Step 2. Results

Step 2 was based on an original steady state torque of about 65% power at 300 MPH. The step input of torque was 52 ft. lbs. or equivalent to roughly an 8% change in power based on the original steady state power at 300 MPH. These percentages varied slightly with change

in speed, due to maintaining constant fuel flow instead of constant torque throughout the speed range. The comments made for Step 1 regarding linear assumptions apply here also.

In this step, derivative control on β was added to the previous requirements of the propeller pitch control to compensate for changes in system response with changes in flight velocity.

From Figure 20, it may be seen that, theoretically, damping ratio, and therefore system response, can be made to approach a constant optimum value for the complete range of flight velocities by the addition of the proper amount of derivative control. The oscillograph traces for this step are presented in Figure 21 through Figure 24, in a form which shows the effect of changing flight velocity at any % D.C.; and also the effect of increasing the % D.C. at any chosen flight velocity. It is seen from these figures that the results agree with those predicted theoretically.

The reduced data for this step is given in Table V, and Figure 26 was drawn from the tabulated values.

From Figure 26, it is seen that by increasing the % D.C., the peak displacement of the variables is decreased for all flight velocities. The advantage of such attenuation are apparent. For instance, by decreasing the transient overshoot of torque, excessive reduction gear loads can be prevented.

It is noted from the response of β , as seen in Figure 23, that very large initial values of propeller pitch velocity and acceleration are indicated, followed by lesser values of propeller pitch velocity. The lesser values of $\frac{d\beta}{dt}$ are indicated in Figure 26. The initial values

of $\frac{d\beta}{dt}$ could not be measured. However, a plot of the change in β at this large initial $\frac{d\beta}{dt}$ is given in Figure 27. By inference, it may be theorized from Figure 27 that the lower the speed and the greater the amount of derivative control, the more extreme the demands or requirements on the propeller control mechanism will be. This particular characteristic of response using derivative control should definitely be investigated further. One way measurements of this phenomena could be easily accomplished with the differential analyzer is by changing the time base.

It is realized that the turbo prop control problem is very complex and has not been solved to anyone's complete satisfaction to date, as is evidenced by the fact that the first production turbo prop system in the United States has only recently been installed in the Navy's XP5Y. This investigation has been based on possibly rudimentary considerations but a sincere attempt has been made to be as general as possible. It is realized that the investigation is not complete and that certain other approaches are desirable, even though not possible to investigate, due to lack of time. A discussion of some of these other considerations follows.

A complete system analysis would necessarily consider the remaining variable not touched upon in this investigation, namely turbine bucket temperature. Such a system, as visualized by the authors, would introduce this variable as a limit to fuel flow rate. What the functional relationship between fuel flow rate and temperature should be or might be has not been investigated. However, it is apparent that rate of change of fuel flow rate must be so limited, regardless of

throttle quadrant movement, to values such that temperature limitations will not be exceeded. In any event, the result would be less stringent than a step input of fuel flow, as is being used in this investigation, and results herein obtained should therefore be conservative.

One basic assumption was to consider rotational speed governed exclusively by propeller blade angle. One problem envisioned in such an assumption would be in the case of simultaneous scheduling of RPM and fuel flow, which is in reality necessary as mentioned in the section on the derivation of propeller data (III C). In this case, an increase in setting of fuel flow and RPM simultaneously would cause an initial decrease in blade angle due to the underspeed condition, resulting in an initially lower rather than higher torque and probably also in more extreme oscillations. A discussion of this is given in Ref. 2.

Propeller blade angle control of RPM is not, however, the only approach possible, although seemingly the most feasible and practicable. An alternate approach as mentioned in Ref. (2), would cause fuel flow to be a function of RPM only, with propeller blade angle controlling the remaining variables.

No time lags, lost motion, or finite limitations on any of the variables were considered. This would be of importance in a physical system where, for instance, a $\frac{d\beta}{dt}$ were required instantaneously with no time allowed for acceleration, but where the propeller governor could only provide a lesser $\frac{d\beta}{dt}$ at a finite acceleration. Other problems would be caused by lost motion in linkages as in the propeller

control mechanism or in the reduction gearing, and also the probability that the fuel pump response would be non-linear and asymptotic to both original and new steady state values of fuel flow.

Such phenomena would have the effect of non-linearizing the system with attendant effect on response. It is considered that, once known, these limitations could be easily set up on the differential analyzer.

Another approach worthy of note would be to make the damping term in the differential equation a function of one or more variables, thereby making the damping variable. For instance, it might be desirable to have low damping for large deviations from steady state and high damping for small deviations from steady state. Such a system is described in Ref. 9, where the damping term is proportional to $1/(a + b|\xi| + c|\dot{\xi}|)$; ξ being the error angle equal to input angle minus output angle $(\theta_i - \theta_o)$. This results in the damping term approaching 1/a at very small deviations from steady state with lesser values at larger deviations. With such a system, very fast response can be obtained with little or no overshoot. Such a system could theoretically be set up for a turbo-prop system as herein analyzed since at steady state,

$$C_{p\beta}\, k_1\, \theta = C_{e_{w_f}}(W_f - W_f^*) = q_{w_f}.$$

Also we know that for this condition, $\theta_o = \theta_i$.

Therefore, changing notation, $\theta_o = \dfrac{q_{w_f}}{C_{p\beta} k_1} = \theta_i$ (at steady state).

This means that the torque input to the system has a simple proportionality relationship to a fictitious θ_i, which can then be

synthetized, enabling one to get ξ since $\xi = \theta_i - \theta_o$. $\dot{\xi}$ would have to be obtained by differentiation. $a + b|\xi| + c|\dot{\xi}|$ and the reciprocal thereof could then be obtained, possibly by using a servo multiplier. This would equal the proportionality constant k_2, getting back to the notation of this investigation. The complete damping term would then be

$$\left[C_{pr_E} - C_{er_E} + \frac{1}{a + b|\xi| + c|\dot{\xi}|} \right].$$

It is not denied that the design of a workable system utilizing these principles would be difficult. Differentiation, integration, addition, subtraction, multiplication, and division of variables would have to be accomplished in the control installation. Presentation of this information, therefore, is intended to show merely what might be accomplished theoretically, using differential analyzer methods.

No effort has been made to indicate any physical hardware which would be necessary to set up an actual control system on any of the premises investigated or discussed, since this investigation deals with investigation, not with design. It is considered, however, that electronic differential analyzer non-linear components could be used in an actual installation, receiving measured variables like rotational speed, blade angle, torque, temperature, and fuel flow. These variables would be operated on, resulting in the formulation of correction signals. As visualized by the authors, one such system would operate with blade angle controlling rotational speed and temperature limiting fuel flow. This would involve a differential analyzer component for the propeller control and one for the fuel regulator. Torque would limit change in

blade angle or fuel flow, or both, as determined to be desirable. Since variable damping gives the best response, this might be incorporated in the propeller control. A movement of the throttle control would then transmit new steady state values of RPM and fuel flow to the propeller control analyzer component and the fuel regulator analyzer component, respectively. Response to these new steady state values would be accomplished in a minimum of time with no danger of exceeding any design limitations.

Such a system would necessarily be complex and probably difficult to maintain and, at present, would be very difficult to design. Such a prospect should not be neglected, however, since it seems to have considerable merit.

SECTION V

CONCLUSIONS AND RECOMMENDATIONS

1. The electronic differential analyzer presents an excellent means for the analysis of the requirements of a control system, such as that for a turbo-prop power plant, in which the complexity and interaction of the variables makes mathematical analysis impractical.

2. The application of an electronic differential analyzer for the control of the turbo-prop power plant should be investigated.

3. The natural-damping of the turbo-prop power plant is insufficient for proper response without augmentation by artificial means.

4. By requiring the propeller pitch control to change pitch at a rate proportional to the engine offspeed and its integral, adequate system response can be obtained for any one operating condition by the proper choice of the prop pitch control proportionality constants. But, at other operating conditions, the response may not be satisfactory.

5. By requiring the propeller pitch control to change pitch at a rate proportional to the engine offspeed, its integral, and its

derivative, a consistent system response at all operating conditions may be approached by the addition of the proper amount of derivative control.

6. The propeller pitch rate and acceleration should be limited to practical values to determine the effect on the response of the control system employed in this investigation.

7. It is recommended that a further investigation of the control system requirements include:

   a. Turbine inlet temperature as a variable.
   b. The effect of control time lags and dead time in the system.
   c. A study of other types of propeller pitch control to determine the optimum type of control, including non-linear requirements.
   d. A study of a system in which a turbine fuel flow governor is used in place of the propeller blade angle governor visualized in this investigation.
   e. A study of the control system response over wide ranges of power utilizing a scheduling procedure of engine speed and fuel flow rate.

SECTION VI

REFERENCES

1. "Automatic Control Considerations for Aircraft Gas Turbine Propeller Power Plants", by C.W. Chilson, G.P. Knapp and M. Meyer: Propeller Division, Curtiss-Wright Corporation, 3 October, 1946. (SAE Preprint)

2. "Designing Turboprop Controls", by George P. Knapp, Project Engineer, Propeller Division, Curtiss-Wright Corporation, 9 January 1950. (SAE Preprint)

3. "Controls for Gas Turbine Propellers", by R.C. Treseder, Aeroproducts Division, General Motor Corporation, 13 April 1948. (SAE Preprint)

4. "Electronic Analog Studies for Turbo-Prop Control Systems", by G.A. Philbrick, W.T. Stark, and W.C. Schaffer, 2 October 1947. (SAE Preprint)

5. "Investigation of the Utility of an Electronic Analog Computer in Engineering Problems", by D.W. Hagelbarger, C.E. Howe, and R.M. Howe: Aeronautical Research Center, Engineering Research Institute, University of Michigan, Ann Arbor, Michigan. External Memorandum No. 28, 1 April 1949.

6. "Performance and Installation Manual", Aircraft Gas Turbine for Propeller Drive, Type TG-100, GEI-19475", General Electric Company, Schenectady, N.Y., 1 November 1944.

7. "Representative Operating Charts of Propellers Tested in the N.A.C.A. 20-Foot Propeller-Research Tunnel", by W.H. Gray and Nicholas Mastrocola, Langley Memorial Aeronautical Laboratory, Langley Field, Va. (ARR NO. 3125), September, 1943.

8. "Airplane Propeller Principles", by W.C. Nelson, 1944, John Wiley and Sons, New York, N.Y.

9. "Nonlinear Damping Investigation", by Ralph I. Berge, College of Engineering Sciences, USAF Institute of Technology, Wright-Patterson Air Force Base, Dayton, Ohio, 15 August 1949.

SECTION VII

SAMPLE CALCULATIONS

Section III C. Selection of Propeller

Determination of V_o/nD and Q_{P_e}:

D = prop. diameter = 10 ft.

i = 11.35

Assume: V_o = 300 MPH = 440 ft/sec

$$n = \frac{13{,}000 \text{ RPM}}{i} = 1145 \text{ RPM} = 19.09 \text{ rev/sec.}$$

$$\rho = 0.002378 \text{ slugs/ft}^3$$

$$\beta = 50^\circ$$

$$V/nD = \frac{440}{(19.09)(10)} = 2.302$$

$$Q_{P_p} = \frac{C_P \rho n^3 D^5}{2\pi n} = \frac{(0.925)(0.002378)(1145^2)(10^2)}{2\pi}$$

$$= 12{,}750 \text{ ft.lbs.}$$

$$Q_{P_e} = \frac{O_{P_p}}{i} = \frac{12{,}750}{11.35} = 1{,}123 \text{ ft.lbs.}$$

Section III E. Evaluation of Constants

$$I_e = 129 \text{ lb. ft.}^2 = 4.008 \text{ slug ft.}^2$$

$$\frac{I_p}{i^2} = \frac{70}{(11.35)^2} = 0.542 \text{ slug ft.}^2$$

$$I_e + \frac{I_p}{i^2} = 4.008 + 0.542 = 4.550 \text{ slug ft.}^2$$

Evaluation of Coefficients for Differential Equations

$$\text{Assuming: } \left.\begin{aligned} V_o &= 300 \text{ MPH} \\ \Omega_e^* &= 13{,}000 \text{ RPM} \\ W_f &= 1400 \text{ lb/hr} \end{aligned}\right\} \text{ Operating Condition}$$

From Figure 4:

$$C_{e_{\Omega_e}} = \left(\frac{\partial Q_e}{\partial \Omega_e}\right)_{W_f} = \frac{-.08 \text{ ft.lbs.}}{\text{rev./min.}} \left(\frac{60}{2\pi}\right) = -0.764 \frac{\text{ft.lbs.}}{\text{rad./sec.}}$$

From Figure 8:

$$C_{P_{\Omega_e}} = \left(\frac{\partial Q_e}{\partial \Omega_e}\right)_{\beta} = \frac{0.28 \text{ ft. lbs.}}{\text{RPM}} \left(\frac{60}{2\pi}\right) = 2.667 \frac{\text{ft.lbs.}}{\text{rad./sec.}}$$

From Figure 11:

$$C_{P_\beta} = \left(\frac{\partial Q_e}{\partial \beta}\right)_{\Omega_e} = \frac{641 \text{ ft. lbs.}}{5 \text{ degrees}} = 128.1 \frac{\text{ft. lbs.}}{\text{degree.}}$$

For Step 1

Assuming: = 0.6

= 5 rad/sec

$$a_2 = I_e + \frac{I_P}{i^2} = 4.55 \text{ slug ft.}^2$$

$$a_0 = \omega_n^2 \, a_2 = 5^2(4.55) = 113.8 \ \frac{\text{slug}^2 \text{ ft.}^4}{\text{sec.}^2}$$

$$a_1 = 2\zeta\sqrt{a_0 a_2} = 2(0.6)\sqrt{(113.8)(4.55)}$$

$$= 27.3 \ \frac{\text{slug}^3 \text{ ft.}^6}{\text{sec.}^2}$$

$$a_0 = C_{P_\beta} k_1$$

$$k_1 = \frac{a_0}{C_{P_\beta}} = \frac{113.8}{128.1} = 0.888$$

$$a_1 = C_{P_{\Omega e}} - C_{e_{\Omega e}} + C_{P_\beta} k_2$$

$$k_2 = \frac{a_1 - C_{P_{\Omega e}} + C_{e_{\Omega e}}}{C_{P_\beta}} = \frac{27.3 - 2.667 + (-0.764)}{128.1} = 0.187$$

For Step 2

Assuming: $\zeta = 0.6$

$\omega_n = 5$ rad/sec.

%D.C. = 200%

$$a_2 = \left[1 + \% D.C.\right]\left[I_e + \frac{I_p}{i^2}\right]$$

$$= \left[1 + 2\right]\left[4.55\right] = 13.65 \text{ slug ft.}^2$$

$$a_0 = \omega_n^2 a_2 = 5^2(13.65) = 341.0 \ \frac{\text{slug}^2 \text{ ft.}^4}{\text{sec.}^2}$$

$$a_1 = 2\zeta\sqrt{a_0 a_2} = 2(0.6)\sqrt{(341.0)(13.65)}$$

$$= 81.9 \ \frac{\text{slug}^3 \text{ ft.}^6}{\text{sec.}^2}$$

$$a_0 = C_{p_\beta} k_1$$

$$k_1 = \frac{a_0}{C_{p_\beta}} = \frac{341.0}{128.1} = 2.66$$

$$a_1 = C_{p_{\Omega e}} - C_{e_{\Omega e}} + C_{p_\beta} k_2$$

$$k_2 = \frac{a_1 - C_{p_{\Omega e}} + C_{e_{\Omega e}}}{C_{p_\beta}} = \frac{81.9 - 2.667 + (-0.764)}{128.1} = 0.615$$

$$C_{p_\beta} k_3 = \left[\% D.C.\right]\left[I_e + \frac{I_p}{i^2}\right]$$

$$k_3 = \frac{\left[\% D.C.\right]\left[I_e + \frac{I_p}{i^2}\right]}{C_{p_\beta}}$$

$$= \frac{(200\%)(4.55)}{128.1} = 0.071$$

Section IV. Reduction of Data from Oscillograph Traces

Example:

Calculation of maximum torque for Step 2 with $\zeta = 0.6$, $\omega_n = 5$ rad/sec, $V_o = 300$ MPH and 200 % D.C.:

Maximum displacement in millimeters from trace = 13.3 MM

Calibration = 20 mm/volt

Attenuation = 100

Multiplication factor = 1 (indicated on Figure 19)

$$q_{max} = (13.3\text{ mm})\ (\text{volt}/20\text{ mm})\ (100)\ (1) = 66.5\text{ volts}$$

$$= 66.5\text{ ft. lbs.}$$

(See Table V)

SECTION VIII

TABLES

	$V_o = 100$ M.P.H					$V_o = 300$ MPH					$V_o = 500$ MPH				
Ω_e RPM	SHP TOTAL	HP FRICTION	SHP_e	w_f Lbs/hr.	Q_e ft. Lbs.	SHP TOTAL	HP FRICTION	SHP_e	w_f Lbs./hr.	Q_e ft. Lbs	SHP TOTAL	HP FRICTION	SHP_e	w_f Lbs./hr.	Q_e ft. Lbs.
13,000	745	81	664	1000	268	1470	84	1386	1300	559	1040	83	957	1000	387
	960	82	878	1100	355	1662	85	1577	1400	636	1280	83	1196	1100	483
	1165	83	1082	1200	437	1860	86	1774	1500	716	1492	85	1407	1200	568
	1360	84	1276	1300	515	2040	87	1953	1600	789	1682	85	1597	1300	645
	1565	85	1480	1400	598	2230	88	2142	1700	865	1870	86	1784	1400	721
	1752	86	1666	1500	674	2418	89	2329	1800	940	2063	87	1976	1500	799
	1944	87	1857	1600	750	2505	90	2415	1850	974	2248	88	2160	1600	873
	2120	88	2032	1700	820						2440	89	2351	1700	950
											2638	90	2548	1800	1030
12,000	594	72	522	900	228	1080	73	1007	1100	440	870	73	797	900	349
	818	72	746	1000	326	1262	74	1188	1200	520	1110	74	1036	1000	454
	990	73	917	1100	401	1438	75	1353	1300	592	1290	75	1215	1100	532
	1165	74	1091	1200	478	1615	75	1540	1400	674	1475	75	1400	1200	613
	1338	75	1263	1300	553	1775	76	1699	1500	744	1655	76	1579	1300	690
	1504	75	1429	1400	625	1940	77	1863	1600	815	1820	77	1743	1400	764
	1665	76	1589	1500	695						2005	78	1927	1500	844
											2162	78	2084	1600	913
											2335	79	2256	1700	987
11,000	650	63	587	900	280	740	64	676	900	323	922	64	858	900	410
	795	64	731	1000	347	890	64	826	1000	394	1080	65	1015	1000	485
	938	64	874	1100	417	1038	65	963	1100	460	1230	66	1164	1100	556
	1080	65	1015	1200	485	1180	66	1114	1200	532	1380	66	1314	1200	628
						1320	66	1254	1300	579	1535	66	1469	1300	702
						1370	66	1304	1340	623	1674	67	1607	1400	768

PERFORMANCE DATA FOR THE T. G. 100

TABLE I.

V_0 MPH	n RPM	V_0/nD	$\beta°$	η %	C_P	Q_{PP} ft. lbs.	Q_{PE} ft. lbs.
100	1145	0.768	20	78	0.13	1790	157.5
			25	73	0.26	3580	315
			30	65	0.42	5790	510
			35	55	0.65	8960	789
			40	50	0.88	12120	1067
			45	40	1.19	16400	1442
	1058	0.832	20	78	0.11	1300	114
			25	75	0.24	2830	249
			30	70	0.40	4720	415
			35	60	0.62	7320	645
			40	50	0.86	10150	893
			45	45	1.17	13800	1213
	969	0.908	20	80	0.08	789	69.5
			25	79	0.20	1970	173.2
			30	75	0.38	3740	329
			35	65	0.59	5810	512
			40	50	0.83	8170	719
			45	45	1.14	11220	987
300	1145	2.302	45	85	0.40	5520	486
			50	85	0.925	12750	1123
			55	79	1.41	19440	1712
	1058	2.494	45	75	0.21	2480	218.5
			50	85	0.78	9210	812
			55	81	1.34	15810	1393
			60	72	1.87	22080	1946
	969	2.723	50	85	0.57	5610	494
			55	83	1.23	12100	1066
			60	77	1.82	17920	1580
500	1145	3.84	55	45	0.12	1653	145.4
			60	81	1.31	18040	1588
			65	78	2.32	31950	2810
	1058	4.15	60	78	1.03	12160	1068
			65	78	2.22	26200	2300
	969	4.53	60	55	0.58	5710	501
			65	80	2.00	19700	1732

PROPELLER DATA

TABLE II.

V_0 MPH	$C_{e_{\Omega_e}}$	$C_{p_{\Omega_e}}$	C_{p_β}	$C_{p_{\Omega_e}} - C_{e_{\Omega_e}}$
100	−0.248	0.954	50.0	1.202
300	−0.372	2.667	128.1	3.039
500	−0.496	4.48	292.0	4.976

Coefficients for Differential Equations

Table III

ζ	a_0	a_1	a_2	k_1	$1/k_1$	k_2	$1/k_2$	ω_n rad/sec.	ω_n CPS	ω rad/sec	ω CPS	q_{w_f} ft Lbs.	$\frac{1}{a_2} = \frac{1}{I_2 + \frac{I_p}{l^2}}$	$\frac{1}{C_{e_{\Omega_e}}}$	$\frac{1}{C_{p_\beta}}$	$\frac{1}{C_{p_{\Omega_e}} - C_{e_{\Omega_e}}}$	CAL. 1V=	ATTN.
1.0	18.2	18.24	4.55	.1419	7.05	.115	8.68	2	.32	2	.32	63.5	.22	-2.79	.0078	.328	10mm	100
1.0	113.8	45.5		.89	1.13	.329	3.04	5	.79	5	.79							
1.0	455	91.1		3.55	.282	.684	1.46	10	1.6	10	1.6							
0.8	19.92	15.24		.1419	7.05	.092	10.83	2	.32	1.25	0.2							
0.8	113.8	36.4		.89	1.13	.257	3.89	5	.79	3.0	.48							
0.8	455	72.8		3.55	.282	.54	1.85	10	1.6	6.0	.96							
0.6	18.2	10.94		.1419	7.05	.059	17.07	2	.32	1.6	.26							
0.6	113.8	27.3		.89	1.13	.187	5.35	5	.79	4.0	.64							
0.6	455	54.6		3.55	.282	.399	2.51	10	1.6	8.0	1.3							
0.3	18.2	5.47		.1419	7.05	.016	63.3	2	.32	1.8	.32							
0.3	113.8	13.65		.89	1.13	.080	12.52	5	.79	4.9	.77							
0.3	455	27.3	V	3.55	.282	.186	5.36	10	1.6	9.9	1.4	Y	Y	V	Y	Y	V	V

		TORQUE							ENGINE SPEED						
ζ	a_0	q_{MAX} mm.	CONVERSION FACTOR	q_{MAX} ft Lbs.	q_{ss} mm.	q_{ss} ft. Lbs	f_q CPS	t_d sec.	CAL 1V=	ATTN	$\Delta\Omega_{e_{MAX}}$ mm.	CONV FACTOR	$\Delta\Omega_{e_{MAX}}$ RPM	f_{Ω_e} CPS	t_d SEC.
1.0	18.2	12.0	10	120	6.4	64		2.33	5mm	10	11.8	1.91	22.5		4.92
1.0	113.8	11.7		117	6.3	63		1.33	20	10	[illegible]	.478	9.0		1.84
1.0	455	11.2		112	6.2	62		.34	20	10	9.6	.478	4.6		6.9
0.8	19.92	12.0		120	6.3	63		3.0	20	100	5.9	.478	28.2		2.8
0.8	113.8	11.8		118	6.3	63		1.6	20	10	[illegible]	.478	10.5		2.2
0.8	455	11.6		116	[illegible]	[illegible]		1.2	20	10	11.9	.478	5.7		1.3
0.6	18.2	12.0		120	6.3	63		4.4	20	[illegible]	7	4.78	33.4		4.4
0.6	113.8	12.0		126	6.6	68	.625	2.13	10	10	[illegible]	.955	12.6	.625	1.6
0.6	455	11.9		119	6.7	67	1	1.3	[illegible]	10	16.1	.637	6.4	1.22	.92
0.3	18.2	12.1		121	6.2	62	.40	10.8	5	10	21.2	1.91	40.5	.31	10.8
0.3	113.8	12.0		125	6.5	65	.62	4.2	10	10	16.9	.955	16.1	.746	4.2
0.3	455	12.0	Y	120	6.3	63	1.47	1.16	[illegible]	[illegible]	17.7	.478	5.5	1.47	1.96

		PROPELLER								PITCH				θ								
ζ	a_0	CAL. 1V=	ATTN.	$\Delta\beta_{MAX}$ mm.	CONV. FACTOR	$\Delta\beta_{MAX}$ °	$\Delta\beta_{ss}$ mm.	$\Delta\beta_{ss}$ °	f_β CPS	t_d sec.	$d\beta/dt$ mm/sec.	$d\beta/dt$ %/sec	$d^2\beta/dt^2$ %/sec²	CAL 5V=	ATTN.	$\Delta\theta_{MAX}$ mm.	CONV. FACTOR	$\Delta\theta_{MAX}$ °	$\Delta\theta_{ss}$ mm.	$\Delta\theta_{ss}$ °	f_θ CPS	t_d sec.
1.0	18.2	20mm.	100	10.3	.05	.515	10	.5		3.5	27.0	1.35		2mm.	0.1	14.7	14.32	210.5	14.7	210.5		5
1.0	113.8			10.8		.54	10	.5		1.72	66.7	3.34		2	0.01	19.2	1.432	27.5	19.2	27.5		1.66
1.0	455			11.0		.55	10	.5		.86	143.0	7.15		2	0.01	5.0	1.432	7.2	5.0	7.2		.84
0.8	19.92			10.8		.54	9.8	.49		3.7	23.5	1.18		2	0.1	13.5	14.32	193.4	13.2	189.0		4.0
0.8	113.8			11.2		.56	9.8	.49		2.3	58.7	2.94		5	0.1	5.2	5.73	29.8	5.1	29.2		1.4
0.8	455			11.5		.575	10.3	.515		0.9	100.0	5.8		5	0.01	15.6	.573	8.9	15.5	8.9		.85
0.6	18.2			11.5		.575	10	.5		4.55	15.0	.75	12.5	2	0.1	15.1	14.32	216.0	14.0	200.5		5.6
0.6	113.8			12.0		.60	10.2	.51	.46	2.2	47.6	2.4		1	0.01	13.9	2.86	39.8	12.9	36.9	.34	2.1
0.6	455			12.2		.61	10.1	.505	.81	1.0	91.0	4.6		3	0.01	9.2	.945	8.7	8.6	8.1	.76	1.0
0.3	18.2			13.7		.685	10	.5	.29	13.0	10.0	0.5	1.0	1	0.1	10.9	28.6	312.0	7.8	223.0	.28	13.0
0.3	113.8			13.9		.695	10	.5	.58	4.2	31.2	1.6	19.5	1	0.01	17.2	2.86	49.2	13.0	37.2	.54	4.2
0.3	455	V	V	14.0	V	.70	9.8	.47	1.37	1.87	62.5	3.1	150	2	0.01	8.7	1.432	12.5	6.3	9.0	1.39	1.87

DATA FOR STEP 1

TABLE IV

																		TORQUE									ENGINE SPEED							PROPELLER						PITCH							θ								
V_0 MPH	%D.C.	ζ	ω_n $\frac{rad}{sec.}$	a_0	a_1	a_2	k_1	$1/k_1$	K_2	$1/k_2$	k_3	$1/k_3$	q_{w_f} ft.Lbs.	$\frac{1}{I_e+\frac{I_p}{i^2}}$	$\frac{1}{C_{e_{\Omega e}}}$	$\frac{1}{C_{p_\beta}}$	$\frac{1}{C_{e_{\Omega e}}-C_{q_{\Omega e}}}$	CAL. 1V =	ATTN	q_{MAX} mm.	CONV. FACTOR	q_{MAX} ft.Lbs	q_{ss} mm.	q_{ss} ft.Lbs	f_q CPS	t_d sec.	CAL 1V =	ATTN	$\Delta\Omega_{e_{MAX}}$ mm	CONV. FACTOR	$\Delta\Omega_{e_{MAX}}$ RPM	$f_{\Omega e}$ CPS	t_d sec	CAL. 1V =	ATTN	$\Delta\beta_{MAX}$ mm	CONV. FACTOR	$\Delta\beta_{MAX}$ °	$\Delta\beta_{ss}$ mm	$\Delta\beta_{ss}$ °	f_β CPS	t_d sec	$\Delta\beta$ $(\frac{d\beta}{dt}\to\infty)$ mm	$\Delta\beta$ $(\frac{d\beta}{dt}\to\infty)$ °	$\frac{d\beta}{dt}$ $\frac{mm}{sec.}$	$\frac{d\beta}{dt}$ $\frac{°}{sec.}$	CAL 1V =	ATTN	$\Delta\theta_{MAX}$ mm	CONV. FACTOR	$\Delta\theta_{MAX}$ °	$\Delta\theta_{ss}$ mm	$\Delta\theta_{ss}$ °	f_θ CPS	t_d sec.
100	0	.375	3.12	44.4	16.67	4.55	.888	1.127	.19	5.28	—	—	36	4.55	4.04	.62	.83	20mm	100	12.8	5	64	7.2	36	.48	3.85	10mm	10	16.	.955	15.6	.46	5.4	10mm	100	11	0.1	1.1	8.1	.81	.44	4.8	0	0	18.7	1.87	10	100	11.5	5.73	60.1	9.0	51.5	.42	4.7
	0	.375	3.12	44.4	10.67	4.55	.888	1.127	.19	5.28	—	—	52									92.5		52							22.5							1.56		1.17			0	0		2.76					86.6		74.1		
	100	.45	3.75	88.7	21.3	6.32	1.78	.564	.40	2.48	.036	28.2								16.0		86	10.2	51	.50	3.0	15	10	20	.635	12.7	.56	3.5	10	100	14.2	0.1	1.42	12	1.2	.48	3.2	3.2	.32	23.2	2.33	20	100	16.5	2.86	47.2	13.8	39.5	.5	3.2
	200	.49	4.06	133.0	31.44	8.1	2.66	.376	.62	1.72	.071	14.1								14.6		73	10.1	50.5	.595	2.4	20	10	[illegible]	.476	9.79	.58	3.4	10	100	13.6	0.1	1.36	11.7	1.17	.50	3.3	5	.50	23.2	2.32	20	100	16.9	2.86	31.9	9.0	25.7	.5	3.3
↓	300	.51	4.25	177.5	42.6	9.9	3.55	.282	.83	1.21	.107	9.39	↓		↓	↓	↓			14.4		72	10.5	52.5	.595	2.2	15	10	11.3	.635	7.17	.59	2.6	10	100	13.0	0.1	1.30	11.5	1.15	.54	2.4	6	.60	21.8	2.18	20	100	8.0	2.86	22.8	6.9	19.7	.47	2.4
300	0	.6	5.0	113.8	27.3	4.55	.888	1.127	.19	5.28	—	—	36		2.64	.0018	.33			12.6		63	7.6	35	.66	3.1	20	10	17.	.476	8.1	.66	3.2	20	100	7.8	.05	.39	6.6	.33	.63	2.2	0	0	27.8	1.39	20	100	7.8	2.86	22.3	7.2	20.6	.63	2.6
	0	.6	5.0	113.8	27.3	4.55	.888	1.127	.19	5.28	—	—	52									91		51							11.7							.56		.48			0	0		2.0					32.2		29.6		
	100	.6	5.0	227.5	54.6	9.1	1.78	.564	.40	2.48	.036	28.2								14.2		71	10.2	51	.625	2.3	20	10	12.7	.476	6.05	.63	2.4	20	100	10.5	.05	.53	9.8	.49	.68	2.4	4.6	.23	20.4	1.02	20	100	6.0	2.86	17.2	5.4	15.4	.63	2.3
	200	.6	5.0	341.0	81.9	13.7	2.66	.376	.62	1.72	.071	14.1								13.3		66.5	10.1	53.5	.625	2.3	20	10	8.8	.476	4.19	.63	2.3	20	100	10.1	.05	.51	9.4	.47	—	1.5	6	.30	12.9	.65	20	100	19.0	.573	10.9	17.2	9.9	—	2.2
↓	300	.6	5.0	455.0	109.1	18.2	3.55	.282	.83	1.21	.107	9.39			↓	↓	↓			12.6		63	10.6	53	.625	1.8	20	10	6.5	.476	3.1	.63	2.8	20	100	9.8	.05	.49	9.5	.48	—	1.8	7	.35	16.6	.53	20	1.0	14.3	.573	8.2	13.0	7.5	—	1.8
500	0	.91	7.56	259.0	60.3	4.55	.888	1.127	.19	5.28	—	—			2.015	.0034	.201			17.8		89	10.3	51.5	1.04	6.9	20	10	13.6	.476	6.48	—	6.9	10	10	22	.01	.22	19.8	.198	—	1.3	0	0	133.4	1.33	10	1.0	33.1	.573	18.9	33.0	18.9	—	1.2
	100	.72	5.9	519.0	122.5	14.9	1.78	.564	.40	2.48	.036	28.2								13.5		67.5	10.4	52	—	1.4	5	1	14.6	.191	2.79	.65	1.5	10	10	20.5	.01	.21	19.7	.197	—	1.2	14	.14	29.4	.294	10	1.0	12.0	.573	6.9	11.5	6.6	—	1.3
↓	200	.66	5.55	776.0	184.5	25.3	2.66	.282	.83	1.72	.071	14.1	↓	↓	↓	↓	↓	↓	↓	11.6	↓	58	10.4	52	—	1.5	10	1	19.3	.096	1.84	.72	2.0	10	10	20.2	.01	.20	19.8	.198	—	1.2	16.3	.16	17.9	.179	10	1.0	17.0	.286	4.9	15.9	4.6	—	2.4

DATA FOR STEP 2

TABLE V

SECTION IX

LIST OF FIGURES

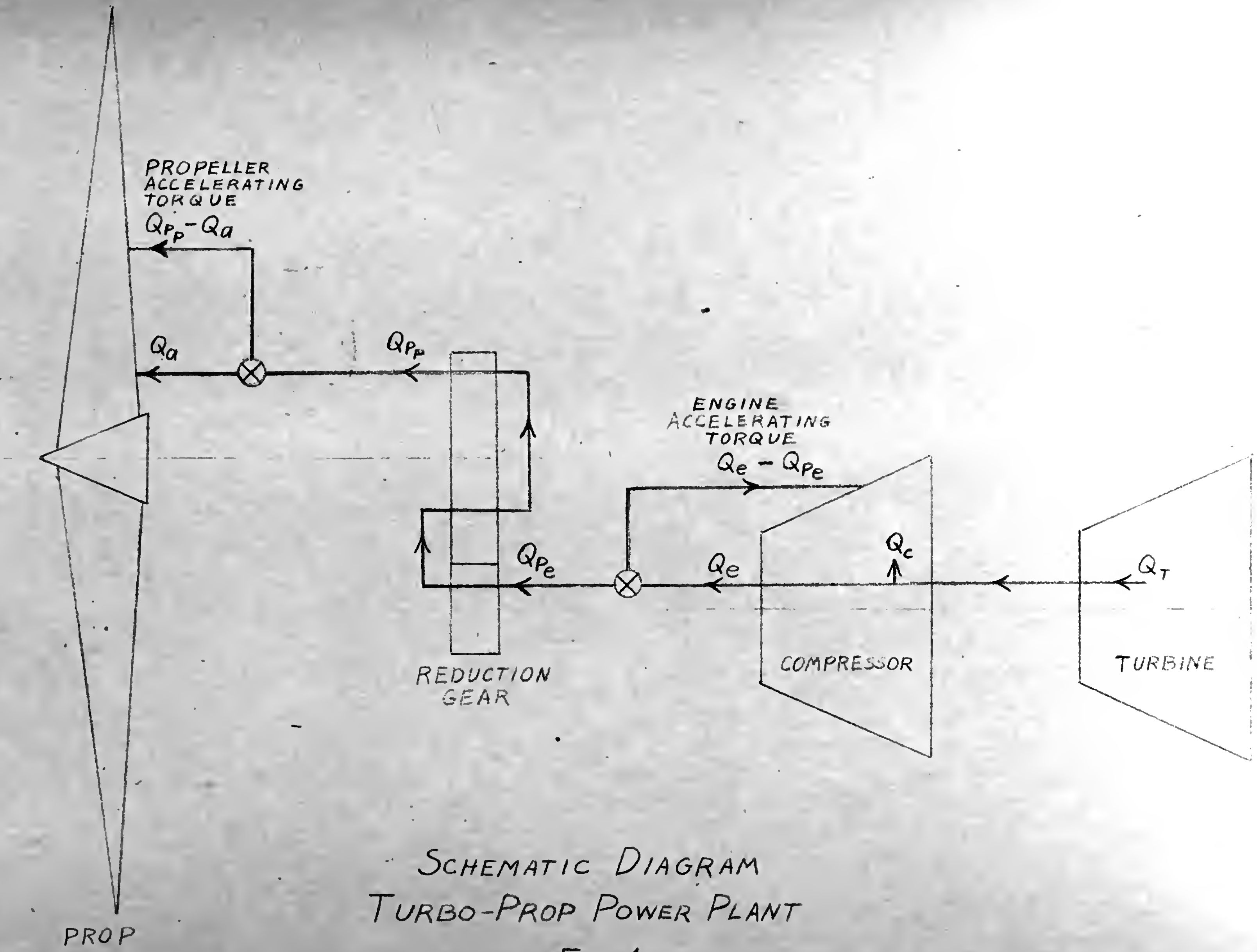

Schematic Diagram
Turbo-Prop Power Plant
Fig. 1

TYPE TG-100 AIRCRAFT GAS TURBINE
FOR PROPELLER DRIVE

PERFORMANCE DATA AT SEA LEVEL

F-2

GAS TURBINE = 13000 RPM
RAM EFFICIENCY = 90%
NACA ATMOSPHERE

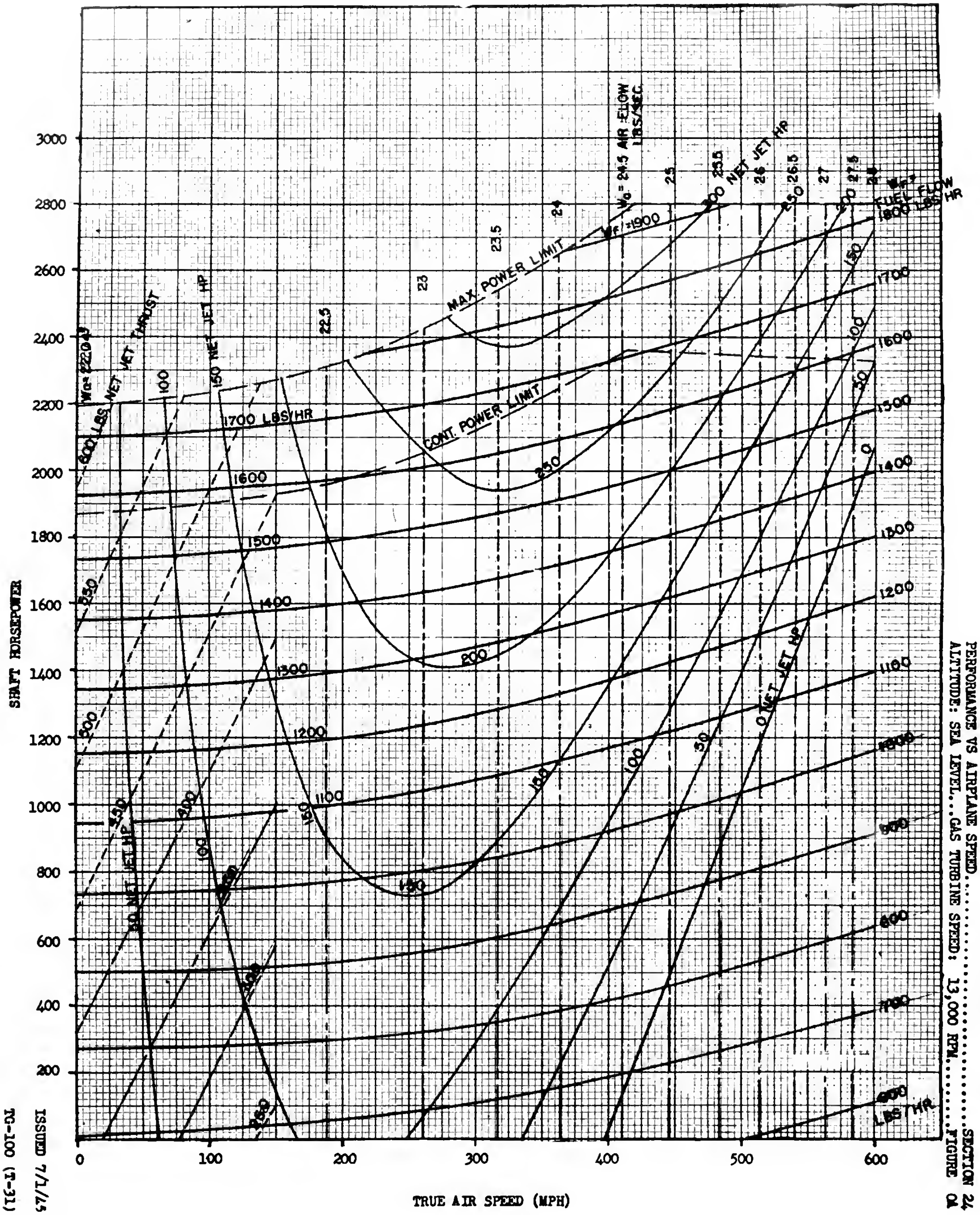

PERFORMANCE VS AIRPLANE SPEED.............................SECTION 24
ALTITUDE: SEA LEVEL...GAS TURBINE SPEED: 13,000 RPM...........FIGURE 02

ISSUED 7/1/45
TG-100 (T-31)

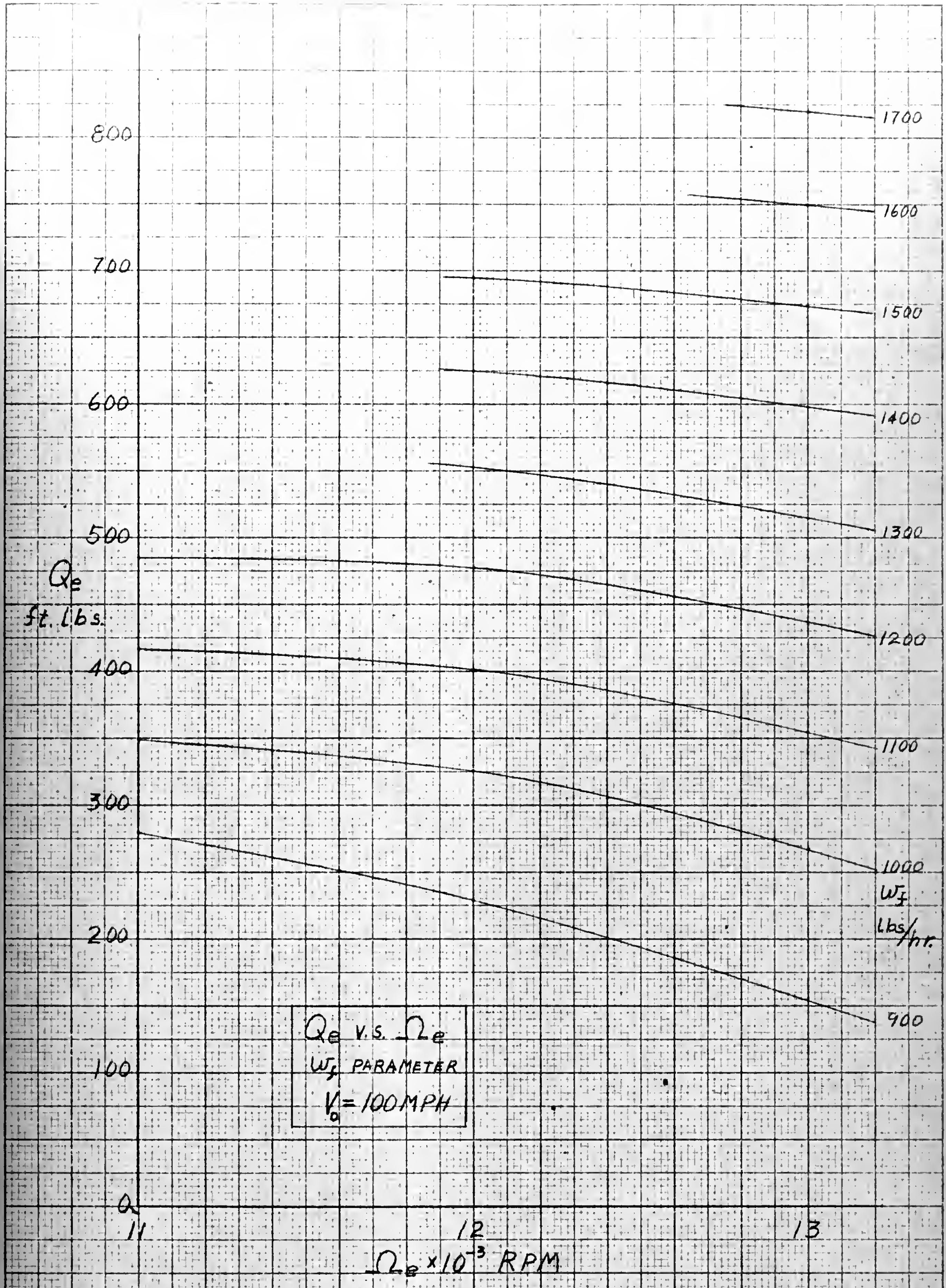
800
700
600
500
Qe
ft. lbs.
400
300
200
100
0
11
12
13
Ωe × 10^-3 RPM
1700
1600
1500
1400
1300
1200
1100
1000
Wf
lbs/hr.
900
Qe v.s. Ωe
Wf PARAMETER
V0 = 100 MPH

FIG. 3

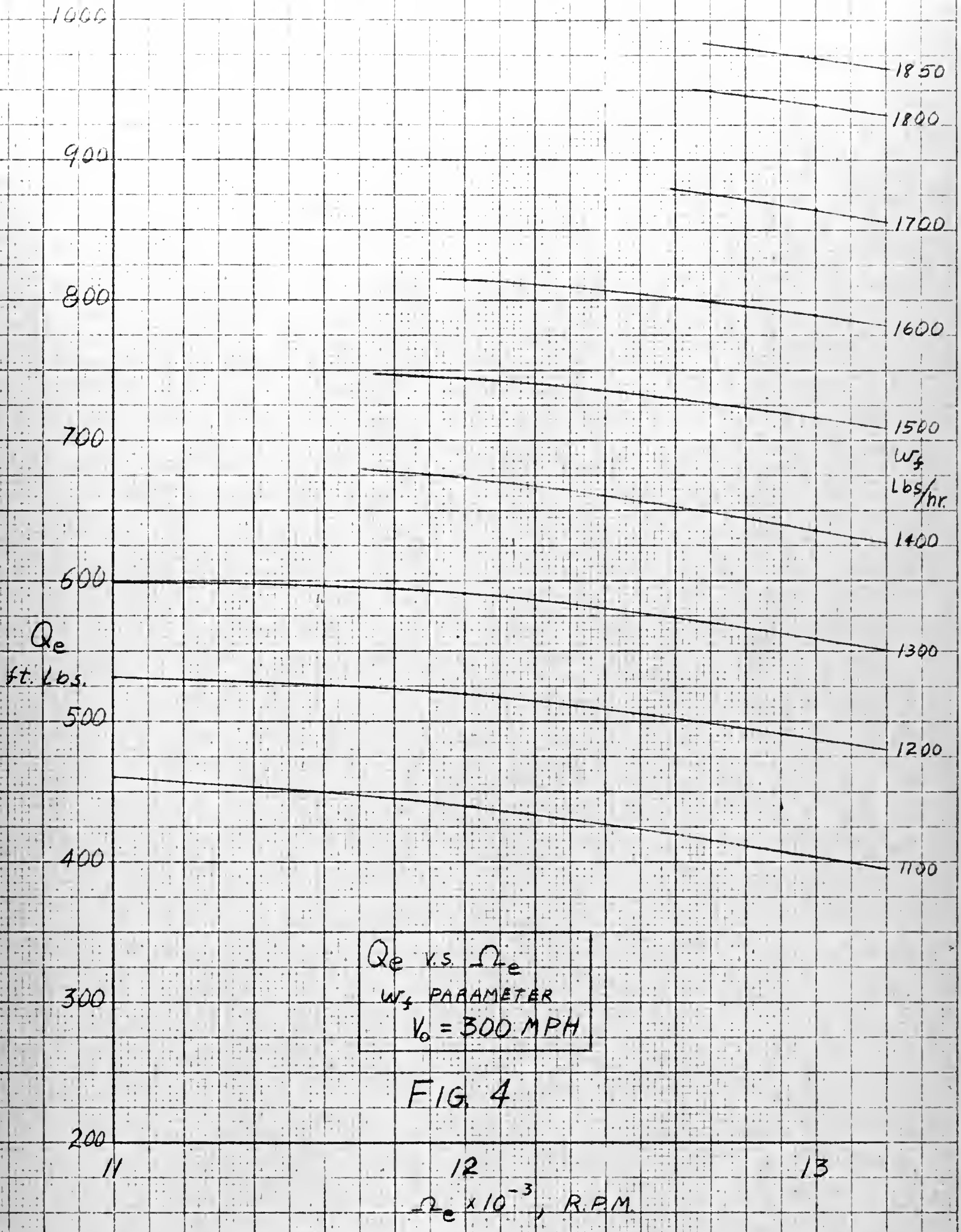
1000
900
800
700
600
500
400
300
200
Qe
ft. Lbs.
1850
1800
1700
1600
1500
Wf
Lbs/hr.
1400
1300
1200
1100
Qe v.s. Ωe
Wf PARAMETER
V0 = 300 MPH
11
12
13
Ωe x10^-3, R.P.M.

FIG. 4

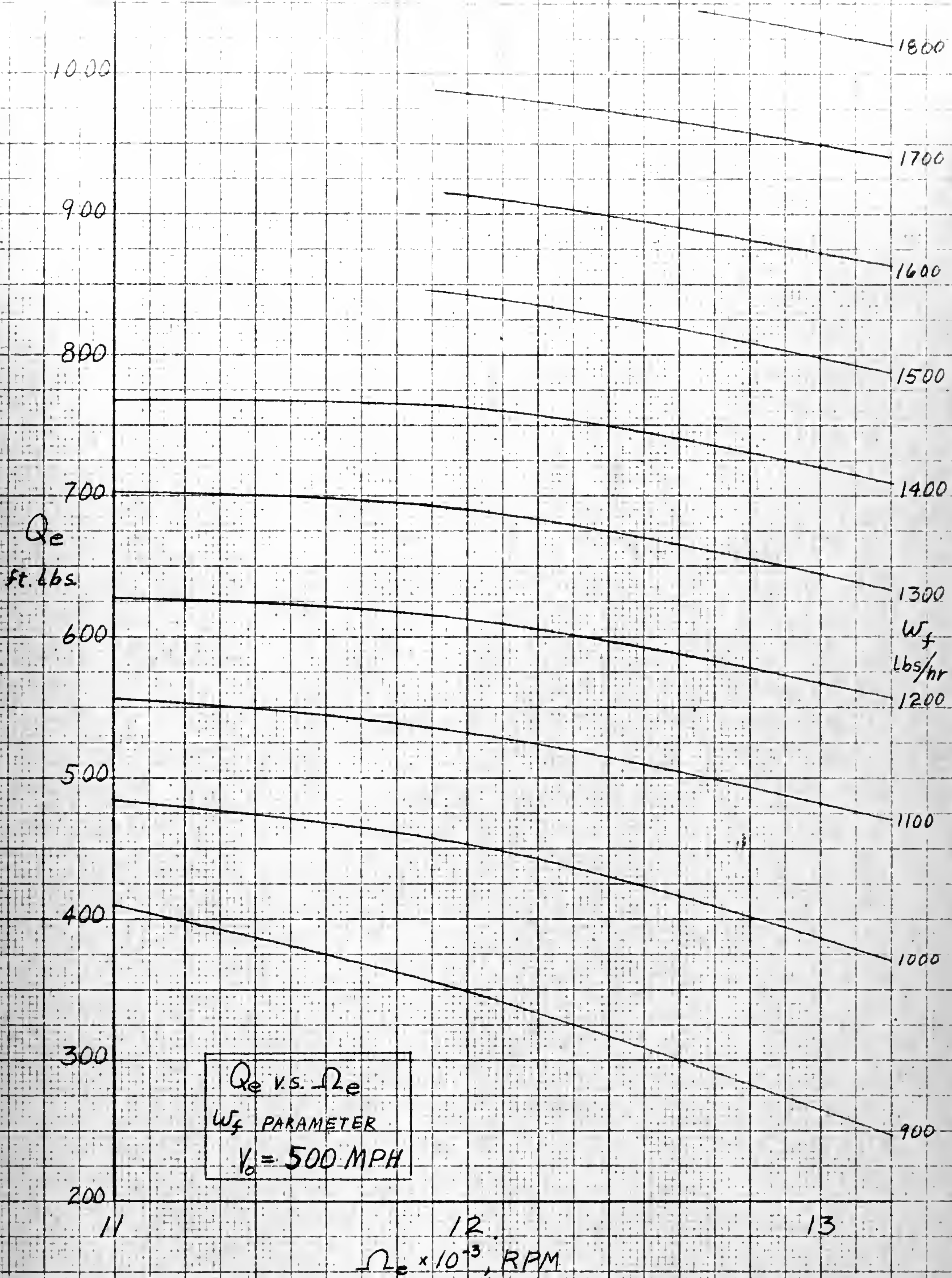
1000
900
800
700
600
500
400
300
200
Q_e ft. lbs.
11
12
13
Ω_e × 10^-3, RPM
1800
1700
1600
1500
1400
1300
1200
1100
1000
900
W_f lbs/hr
Q_e vs. Ω_e
W_f PARAMETER
V_o = 500 MPH

FIG. 5

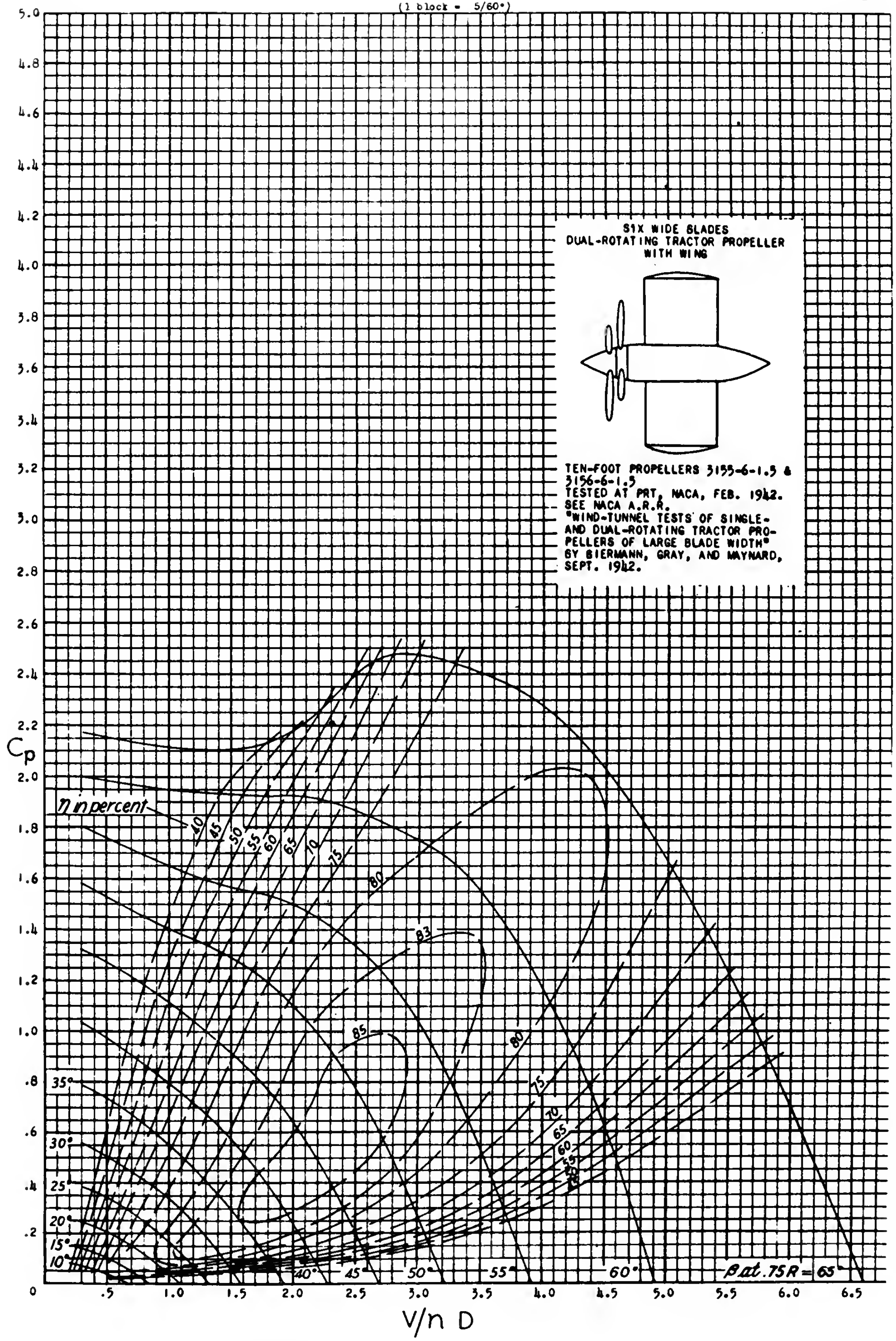
(1 block = 5/60°)
SIX WIDE BLADES
DUAL-ROTATING TRACTOR PROPELLER
WITH WING
TEN-FOOT PROPELLERS 3155-6-1.5 & 3156-6-1.5
TESTED AT PRT, NACA, FEB. 1942.
SEE NACA A.R.R.
"WIND-TUNNEL TESTS OF SINGLE- AND DUAL-ROTATING TRACTOR PROPELLERS OF LARGE BLADE WIDTH"
BY BIERMANN, GRAY, AND MAYNARD,
SEPT. 1942.
Cp
η in percent
40
45
50
55
60
65
70
75
80
83
85
80
75
70
65
60
55
50
45
35°
30°
25°
20°
15°
10°
40°
45°
50°
55°
60°
β at .75R = 65°
5.0
4.8
4.6
4.4
4.2
4.0
3.8
3.6
3.4
3.2
3.0
2.8
2.6
2.4
2.2
2.0
1.8
1.6
1.4
1.2
1.0
.8
.6
.4
.2
0
.5
1.0
1.5
2.0
2.5
3.0
3.5
4.0
4.5
5.0
5.5
6.0
6.5
V/n D

FIG. 6

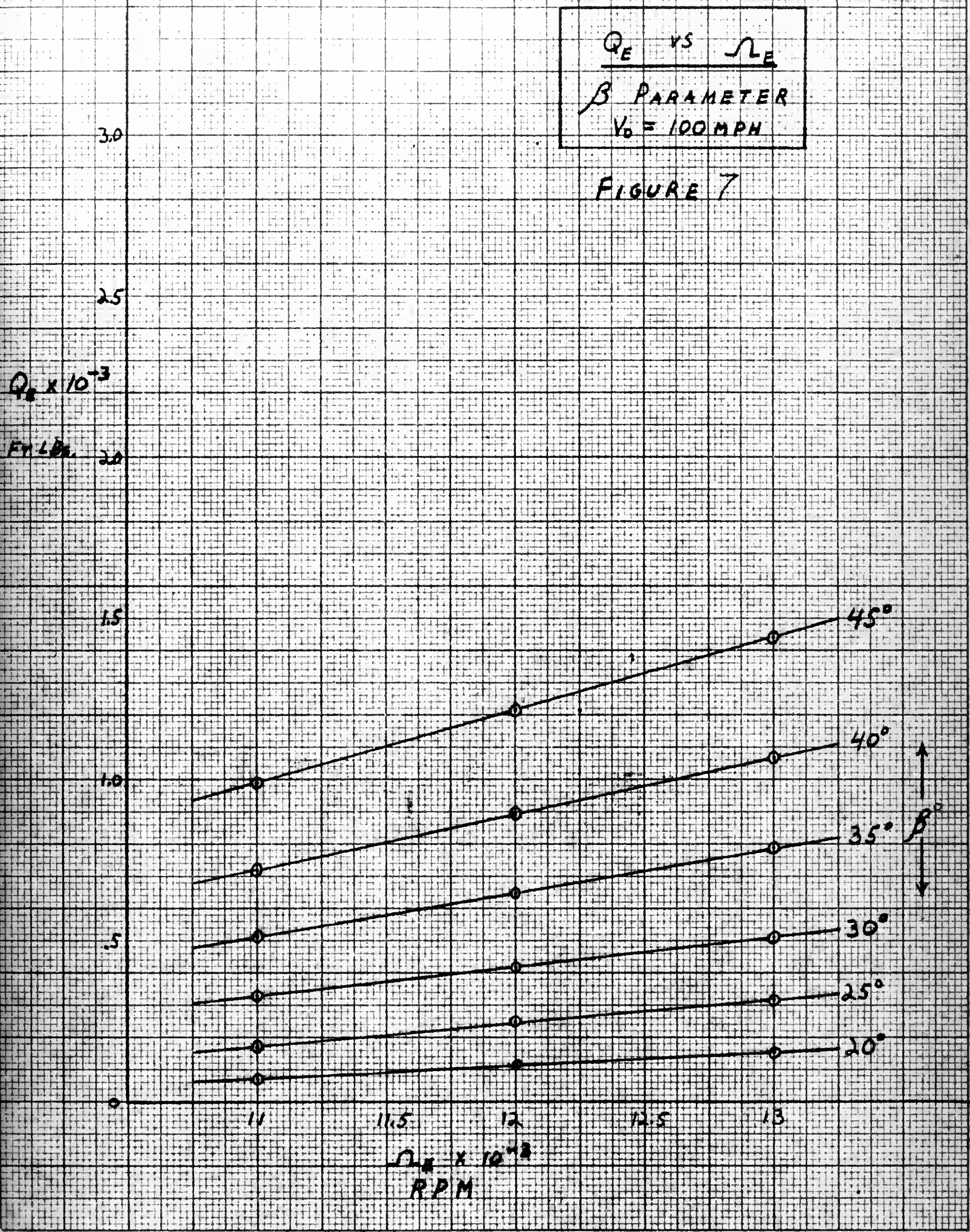

FIGURE 7

Q_E vs Ω_E
β PARAMETER
V_0 = 100 MPH
$Q_E \times 10^{-3}$
FT LBS.
3.0
2.5
2.0
1.5
1.0
.5
0
11
11.5
12
12.5
13
$\Omega_E \times 10^{-2}$
RPM
45°
40°
35°
30°
25°
20°
β°

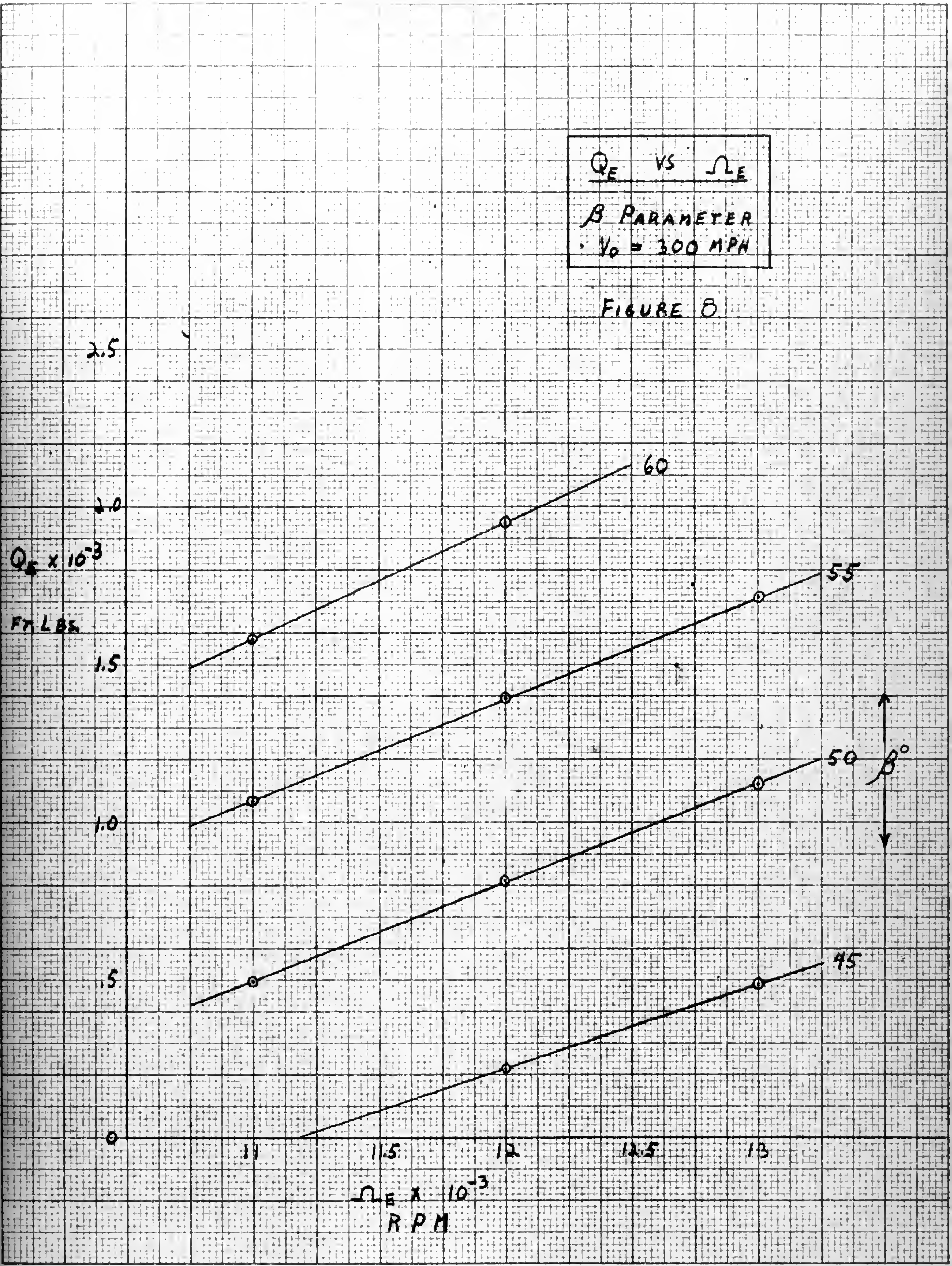

Q_E VS Ω_E

β PARAMETER

$V_0 = 300$ MPH

FIGURE 8

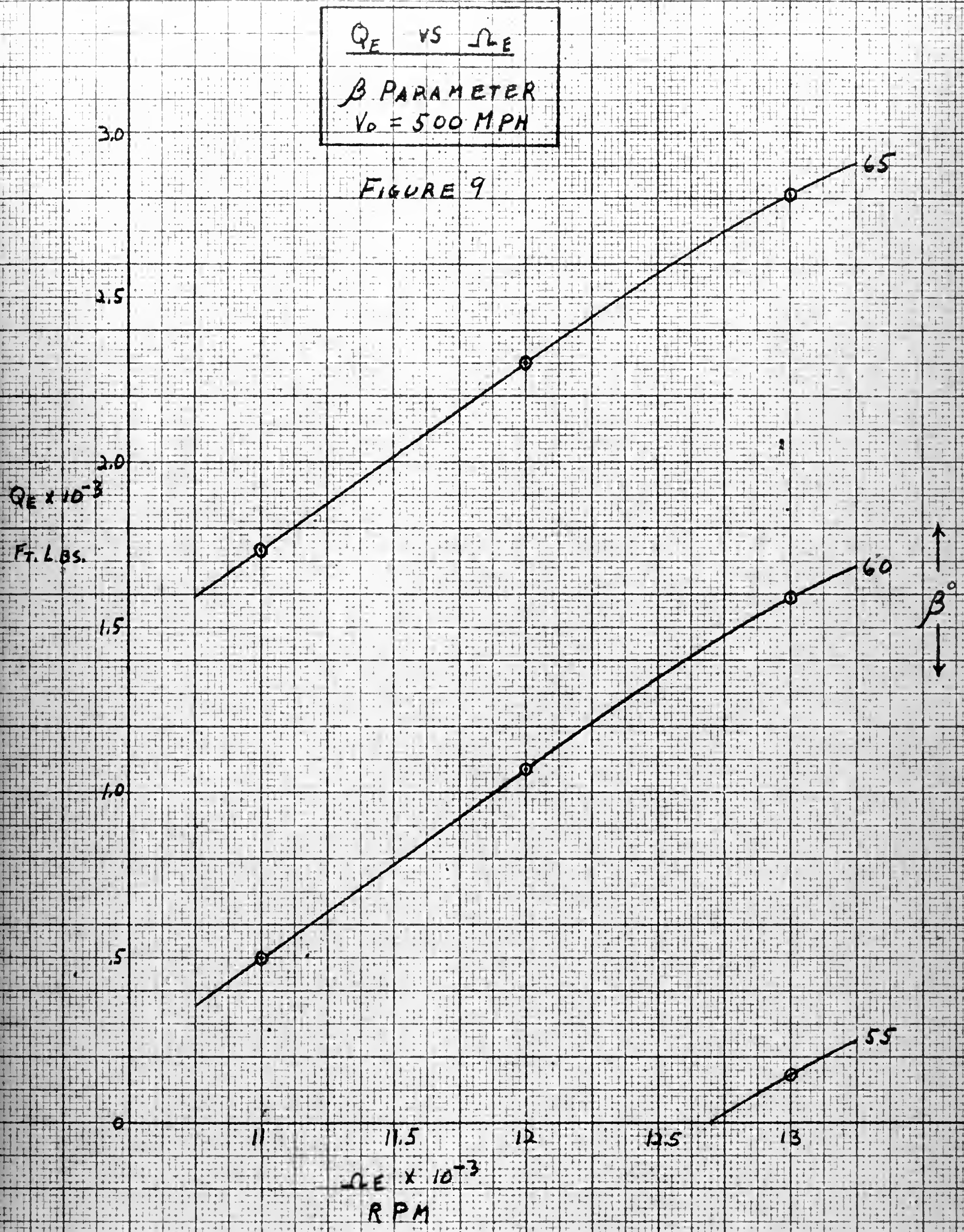
Q_E VS Ω_E
β PARAMETER
V_0 = 500 MPH
3.0
2.5
2.0
1.5
1.0
.5
0
$Q_E \times 10^{-3}$
FT. LBS.
65
60
55
β°
11
11.5
12
12.5
13
$\Omega_E \times 10^{-3}$
RPM

FIGURE 9

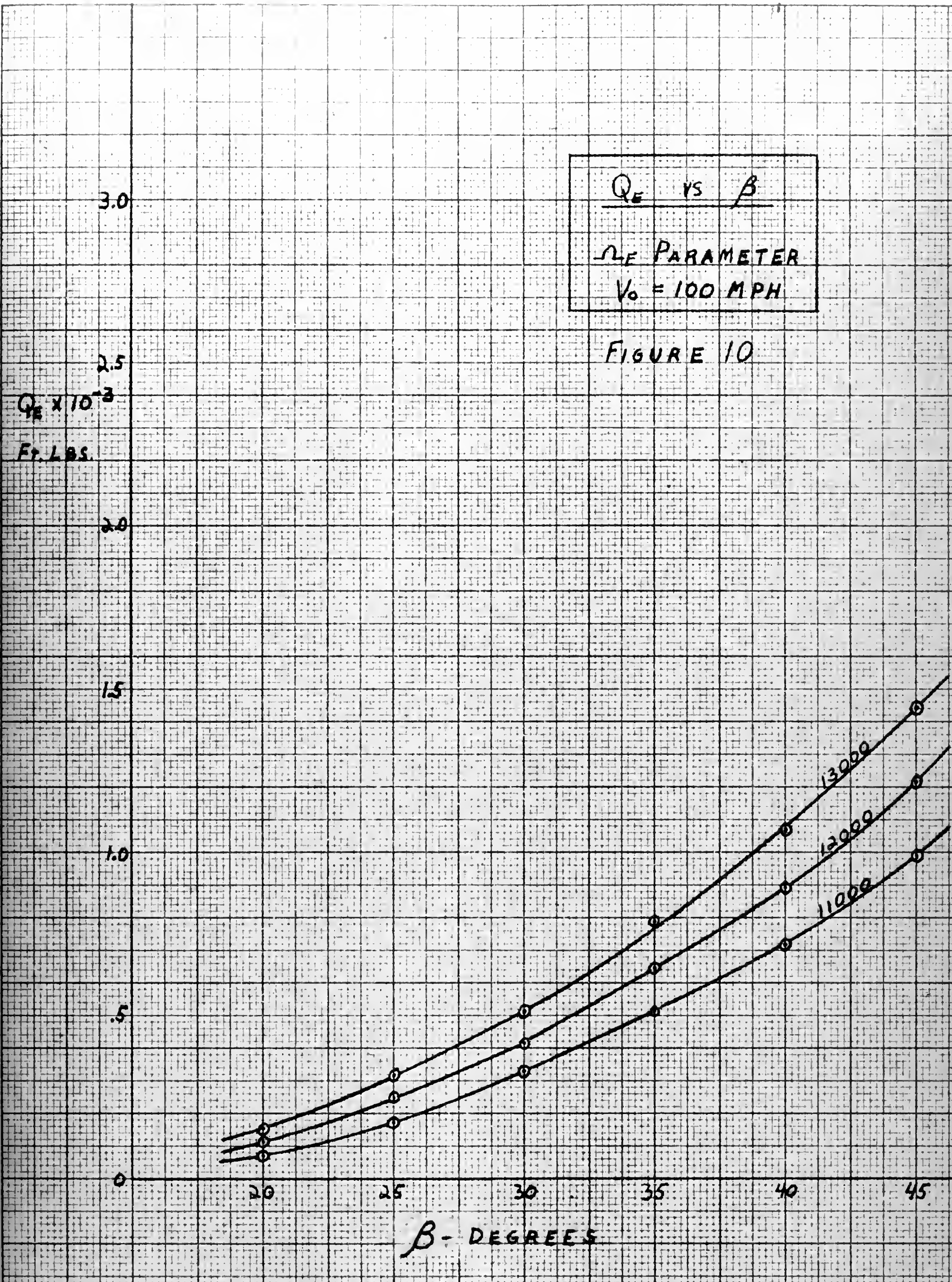
Q_E vs β
Ω_E Parameter
V_0 = 100 MPH
3.0
2.5
$Q_{TE} \times 10^{-3}$
Ft. Lbs.
2.0
1.5
1.0
.5
0
20
25
30
35
40
45
β - DEGREES
13000
12000
11000

FIGURE 10

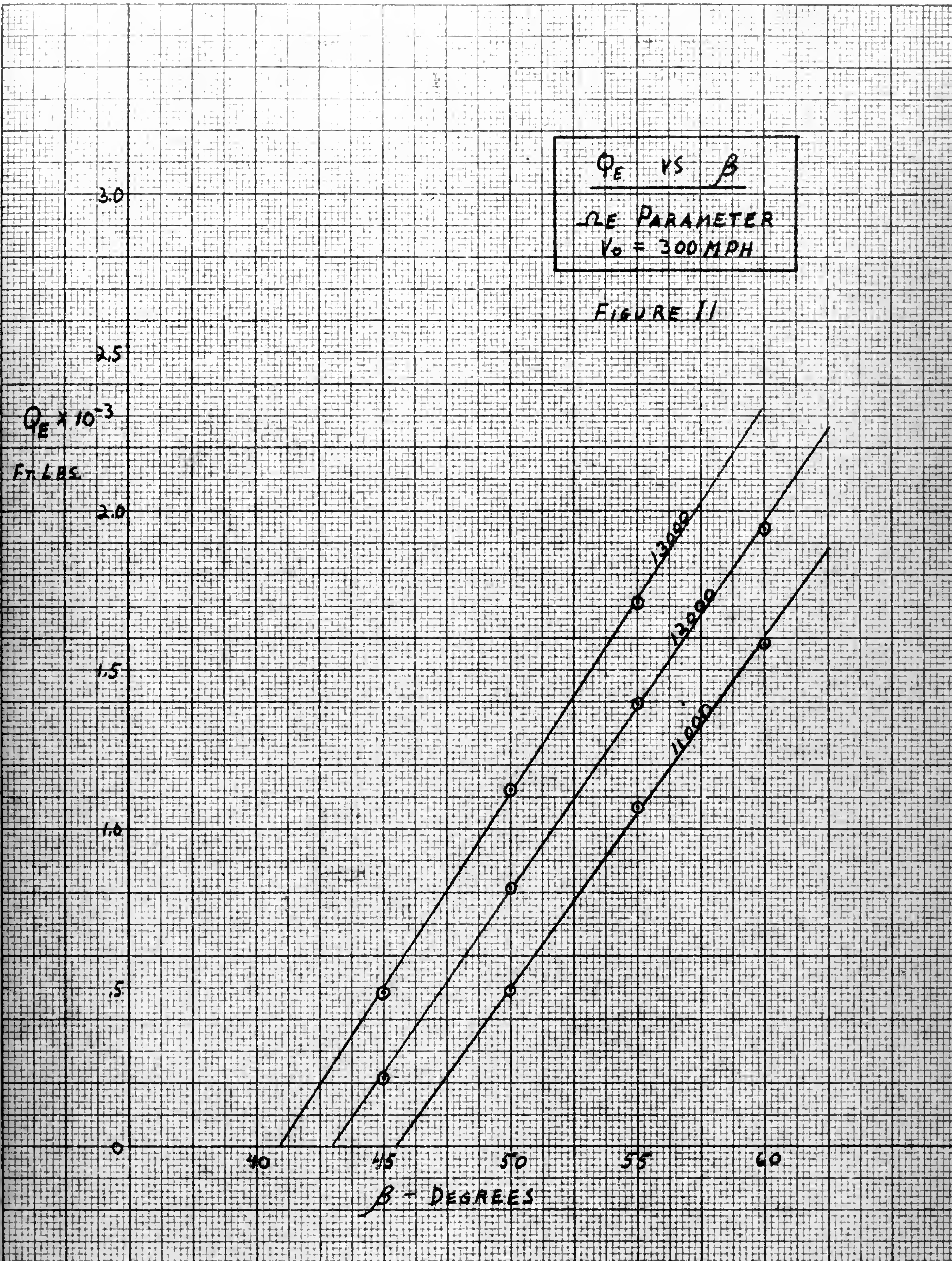

φ_E VS β

Ω_E PARAMETER
V_0 = 300 MPH

FIGURE 11

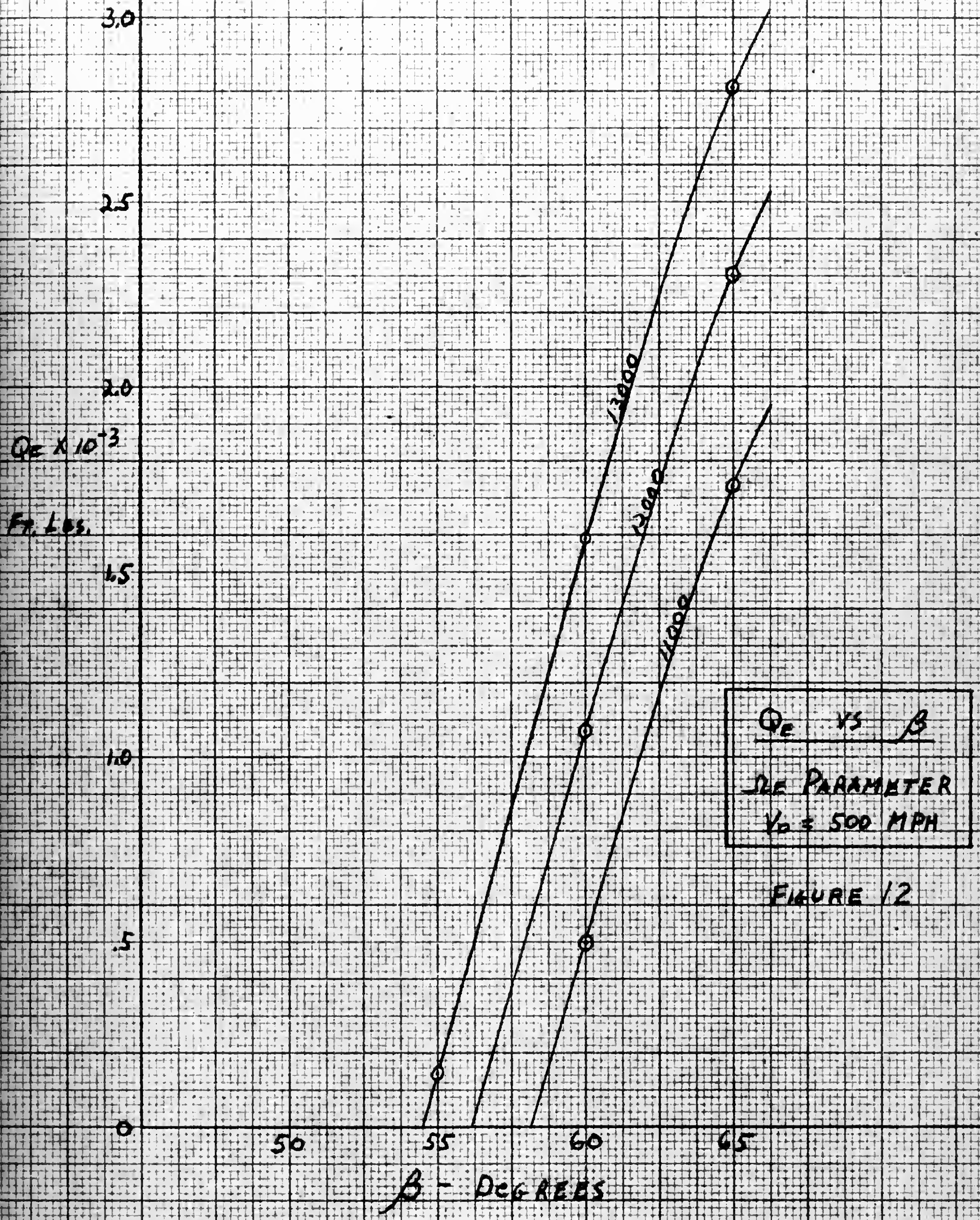
QE VS β
ΩE PARAMETER
VD = 500 MPH
QE X 10^-3
FT. LBS.
3.0
2.5
2.0
1.5
1.0
.5
0
50
55
60
65
β - DEGREES
13,000
12,000
11,000

FIGURE 12

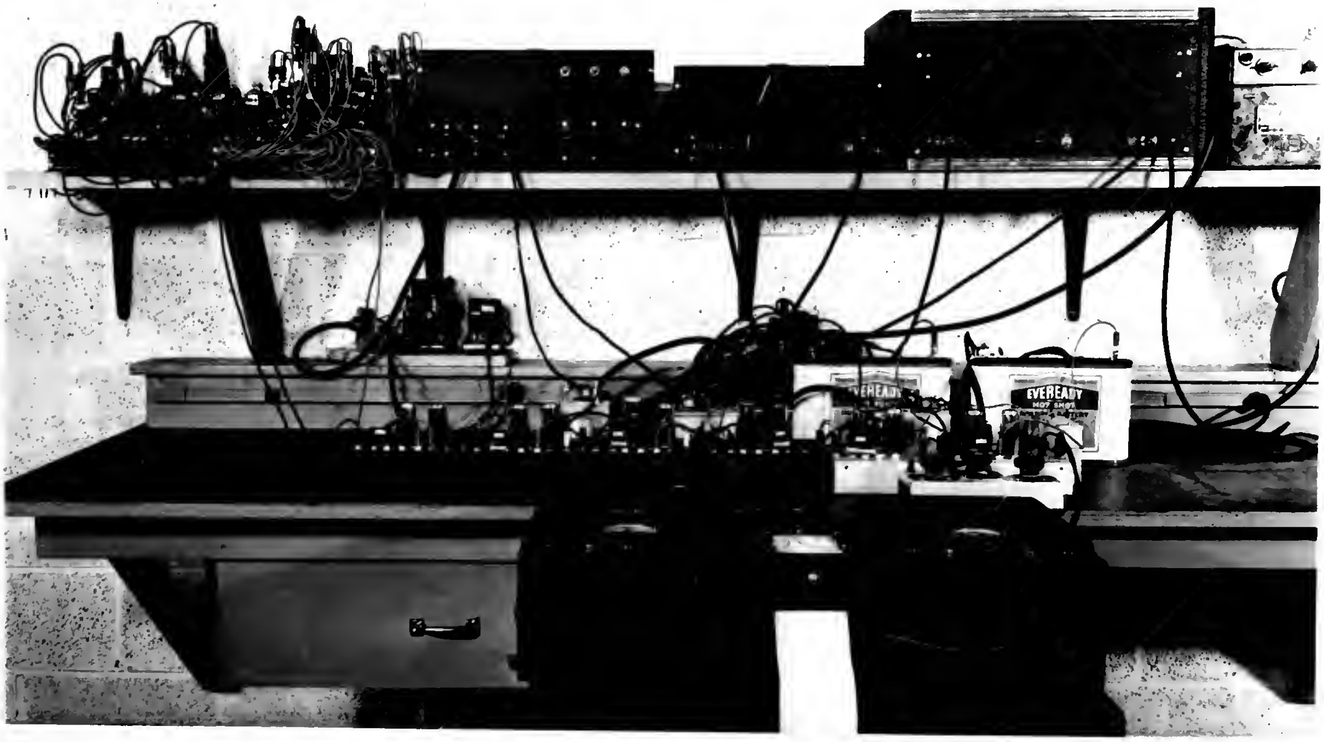

Typical Electronic Differential Analyzer Set-up.

Figure 13

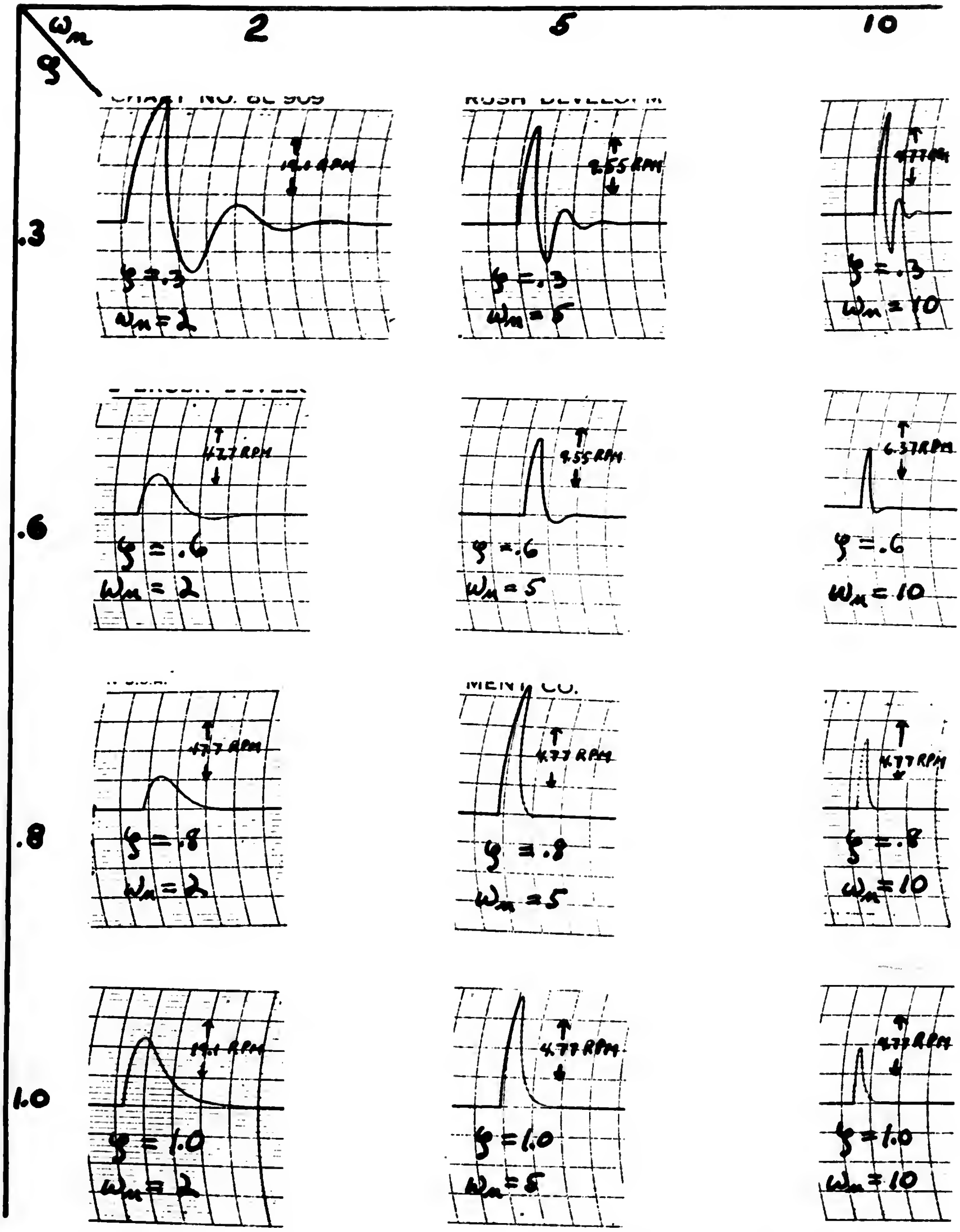

Oscillograph Solutions of Variable ($\Omega_e - \Omega_e^*$)
Step 1.

Figure 14.

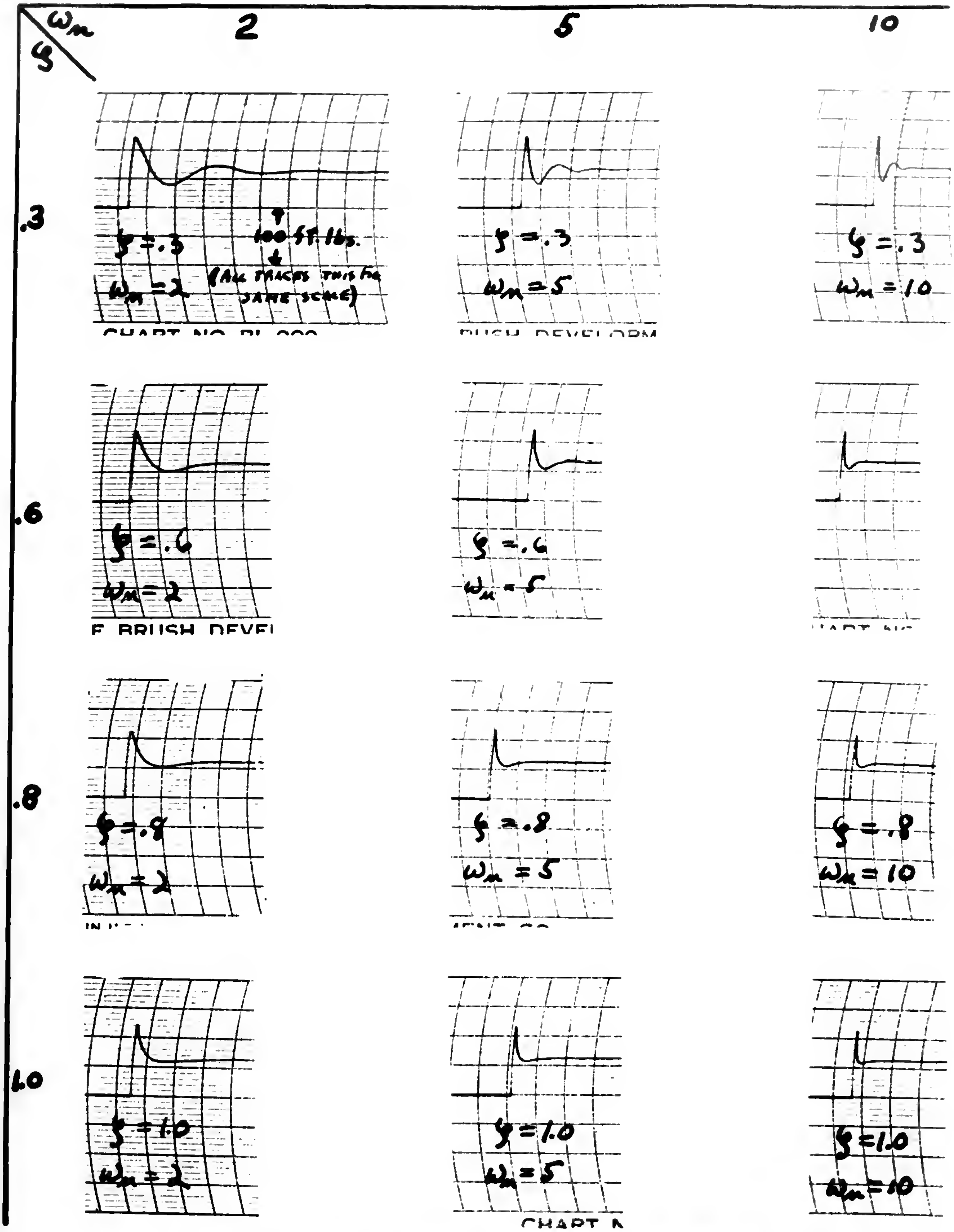

Oscillograph Solutions of Variable $(Q_a - Q_c^*)$
Step 1

Figure 15.

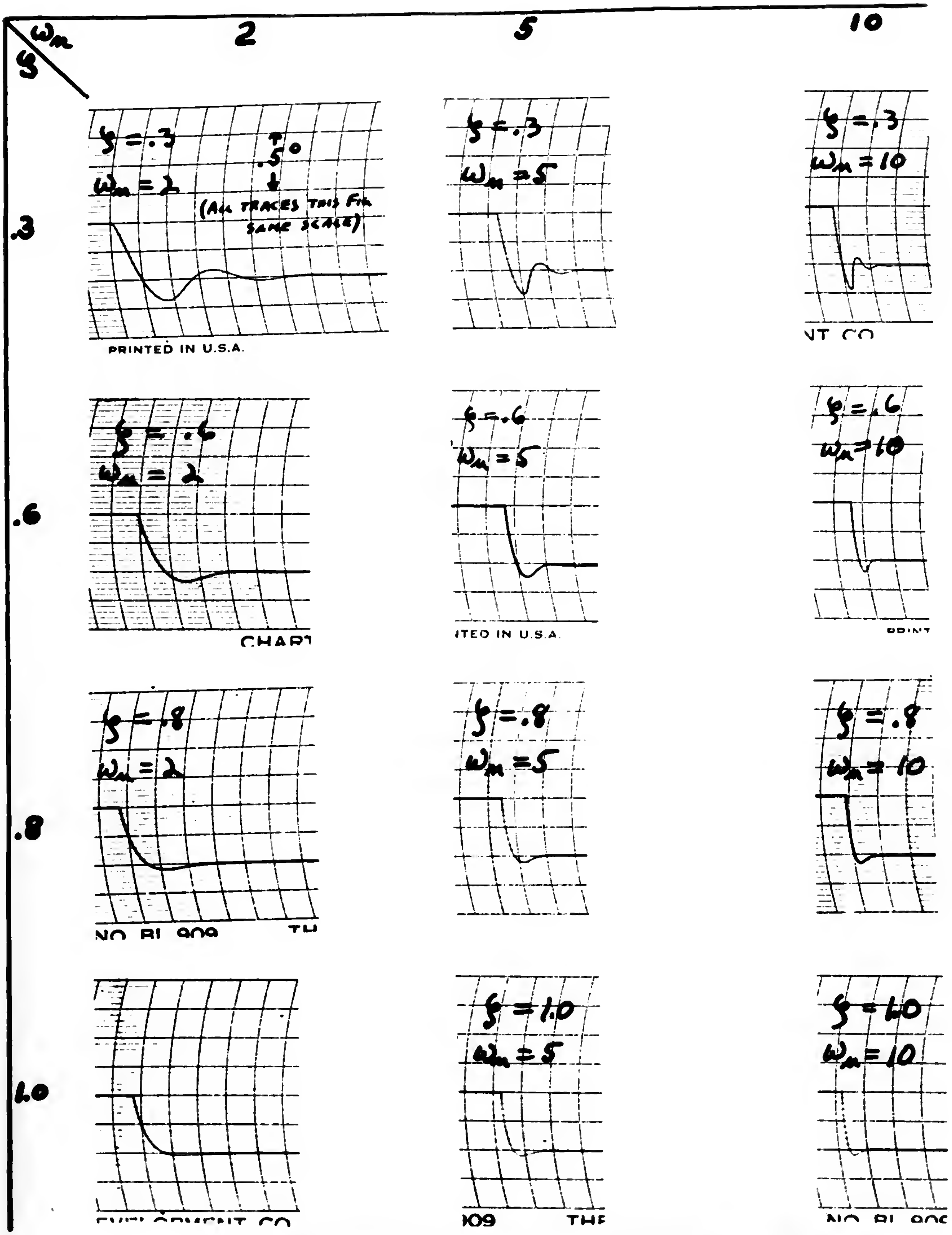

Oscillograph Solutions of Variable $(\beta-\beta^{*})$
Step 1.

Figure 16.

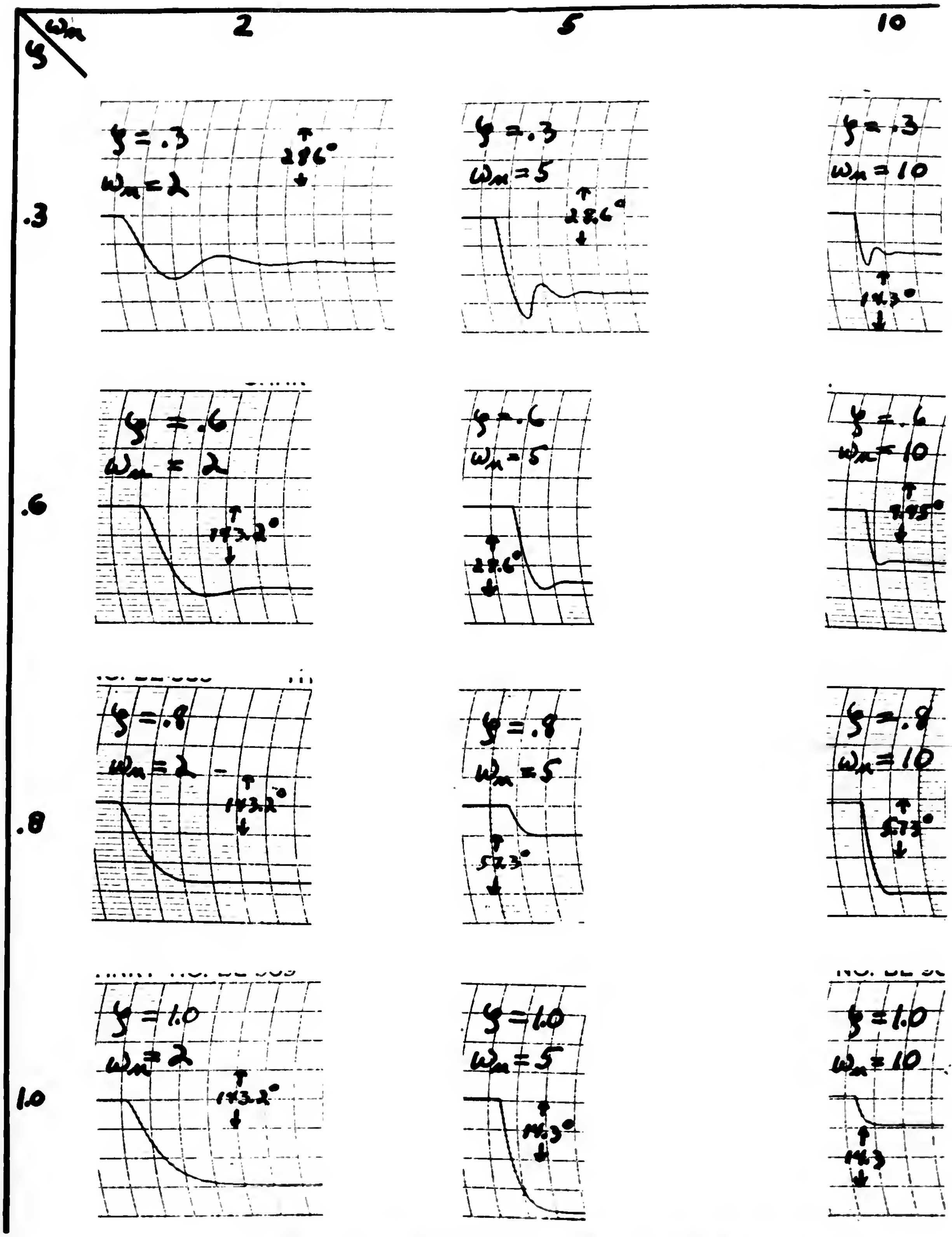

Oscillograph Solutions of Variable (θ).
Step 1.

Figure 17.

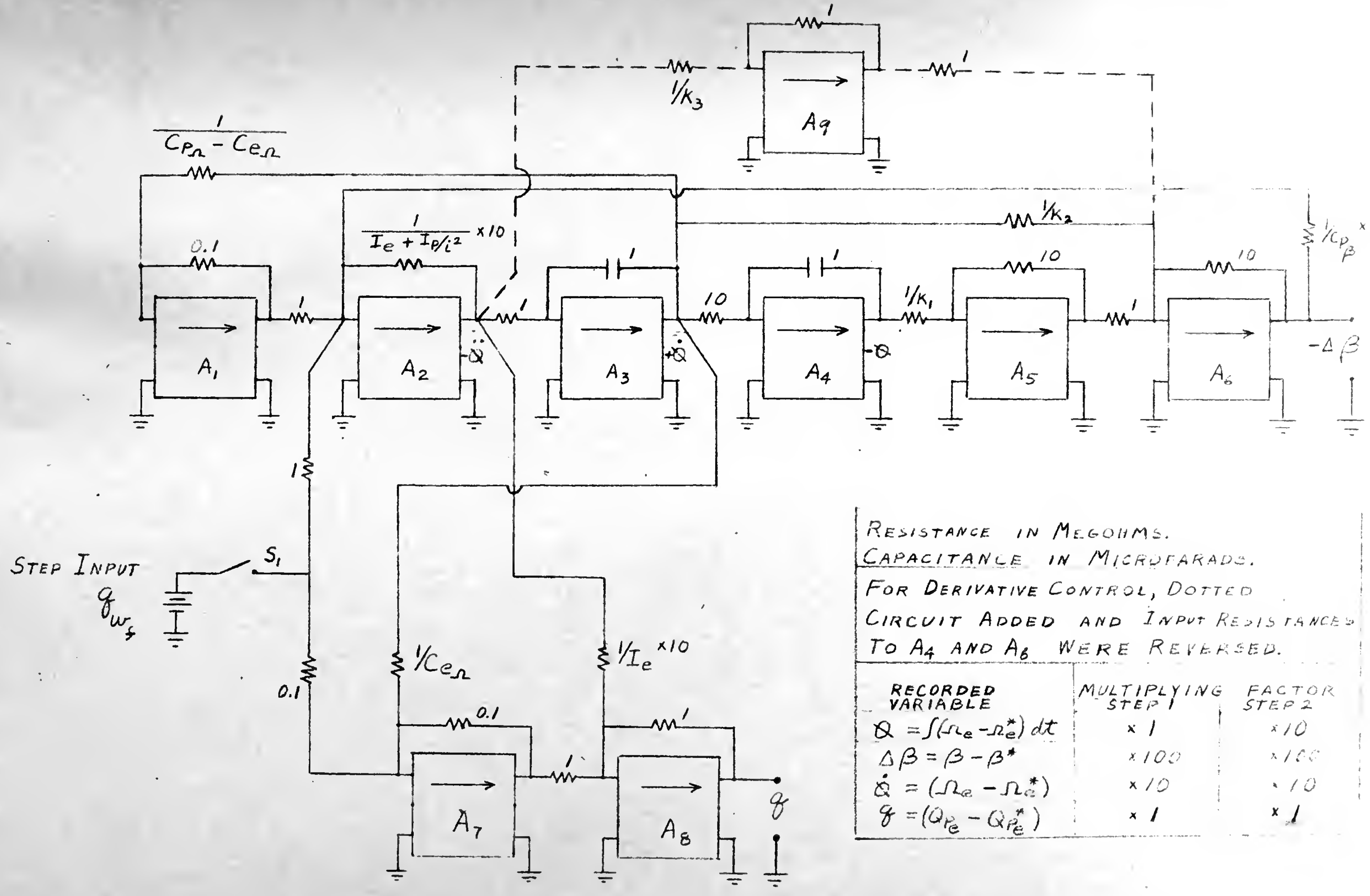

Resistance in Megohms.
Capacitance in Microfarads.

For Derivative Control, Dotted Circuit Added and Input Resistances To A_4 and A_6 Were Reversed.

Recorded Variable	Multiplying Step 1	Factor Step 2
$Q = \int(\Omega_e - \Omega_e^*)\,dt$	×1	×10
$\Delta\beta = \beta - \beta^*$	×100	×100
$\dot{Q} = (\Omega_e - \Omega_e^*)$	×10	×10
$q = (Q_{P_e} - Q_{P_e}^*)$	×1	×1

Differential Analyzer Circuit Diagram Fig. 18

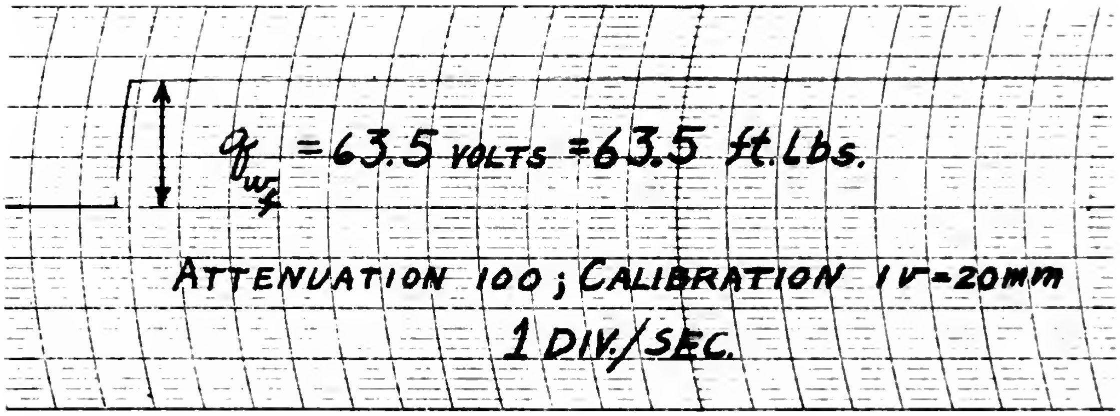

Oscillograph Record of a Typical Step Input.

Fig. 19

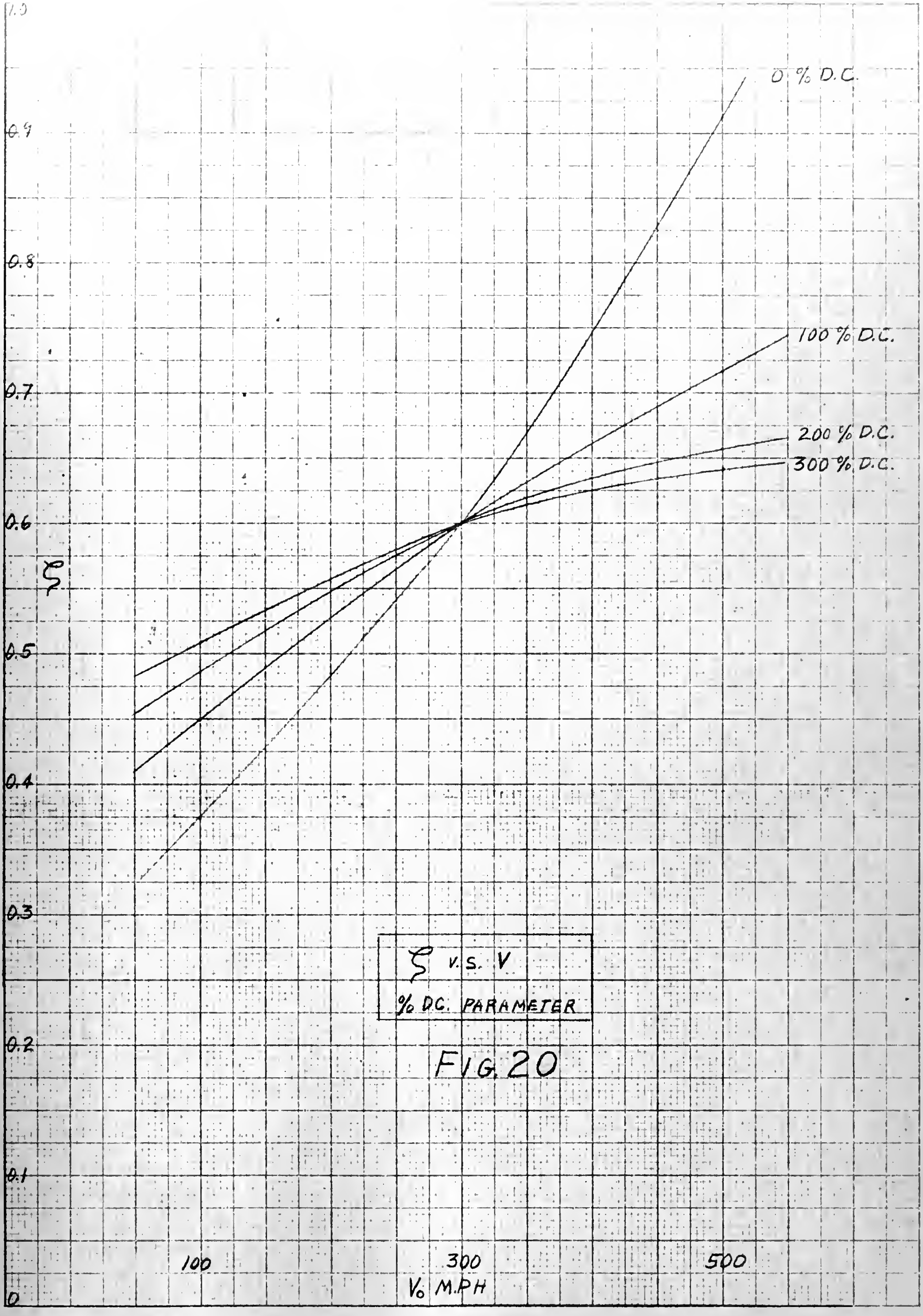

ς V.S. V

% D.C. PARAMETER

FIG. 20

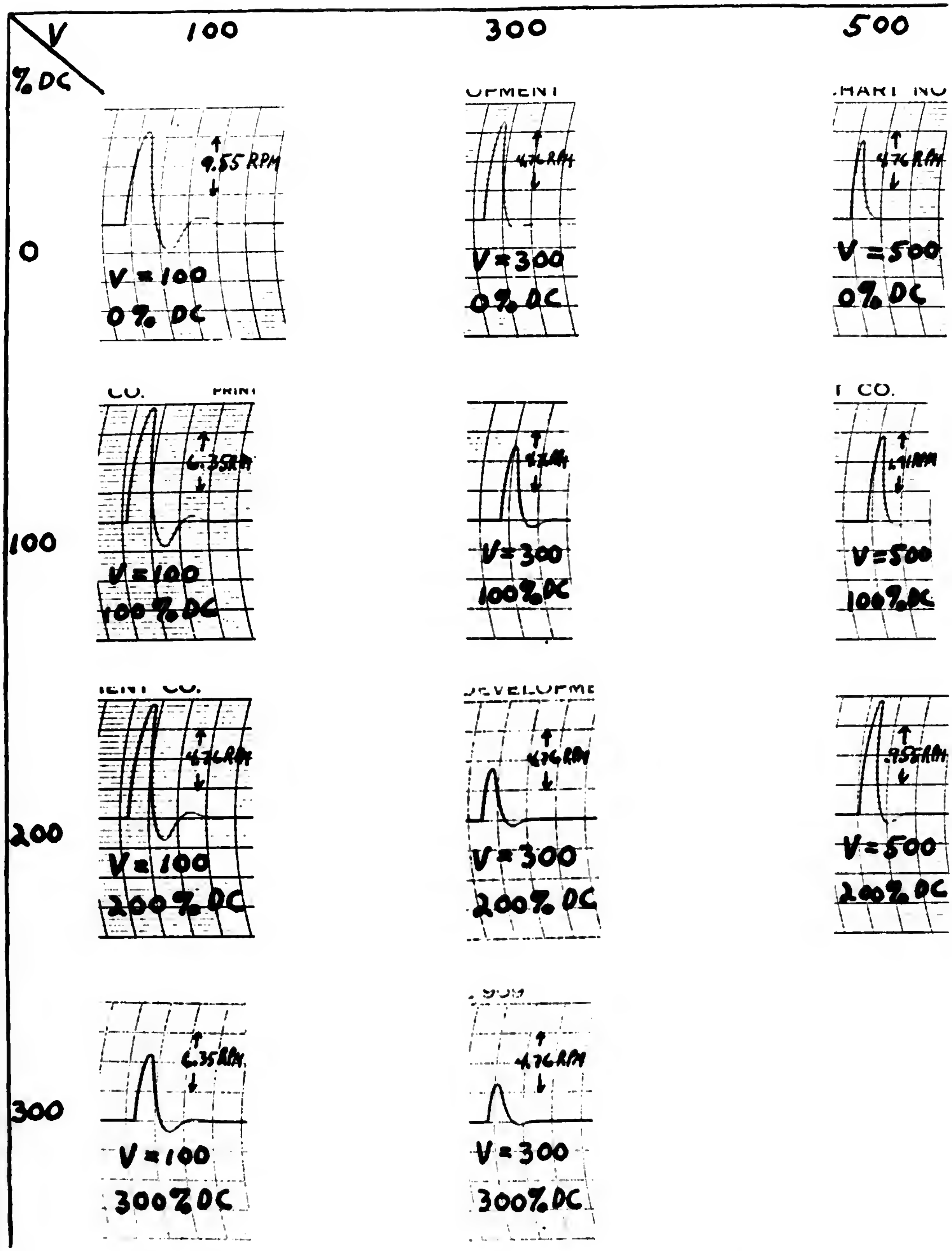

Oscillograph Solutions of Variable $(\Omega_2 - \Omega_2^*)$
Step 2.

Figure 21.

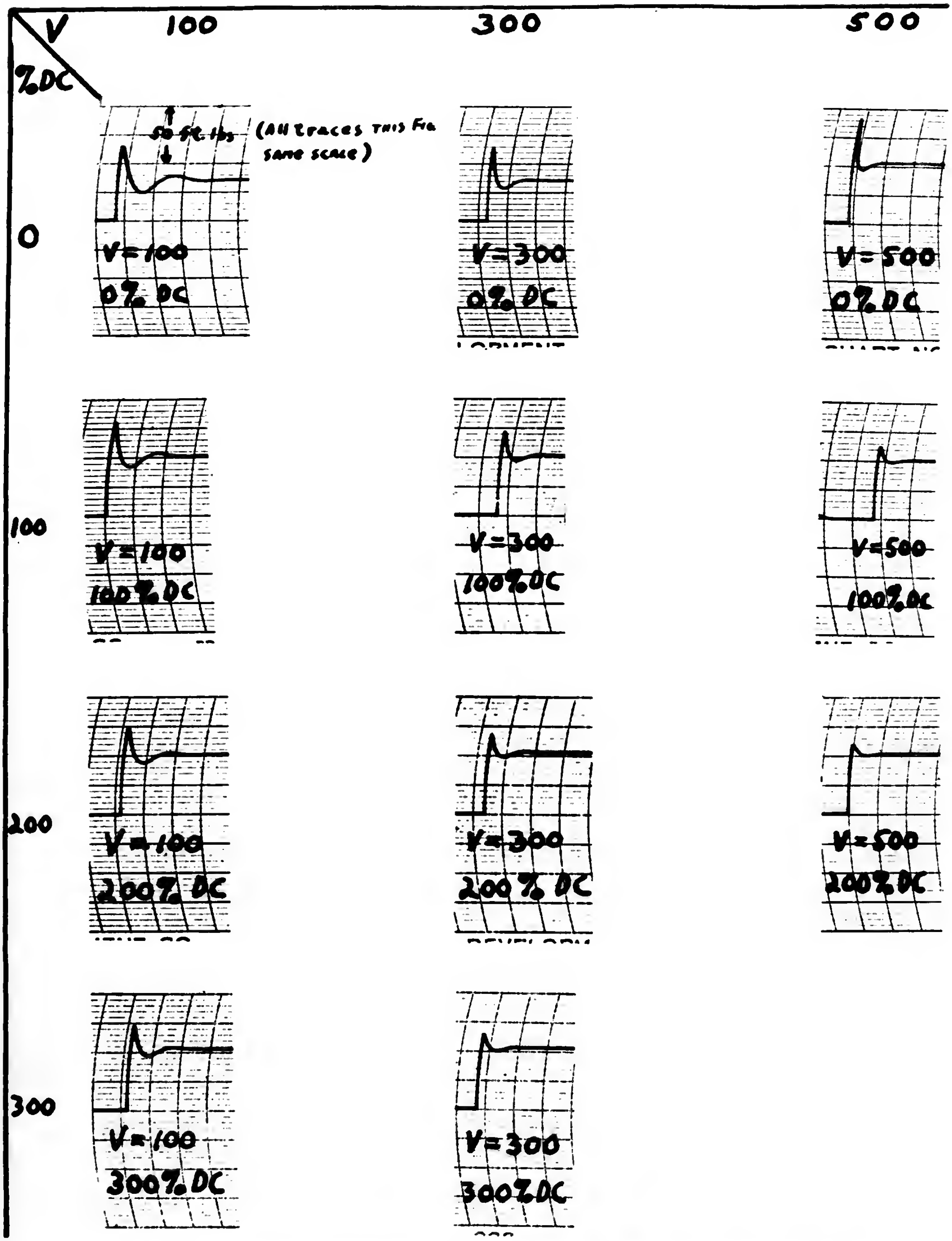

Oscillograph Solutions of Variable ($Q_c - Q_c^*$)
Step 2.

Figure 22.

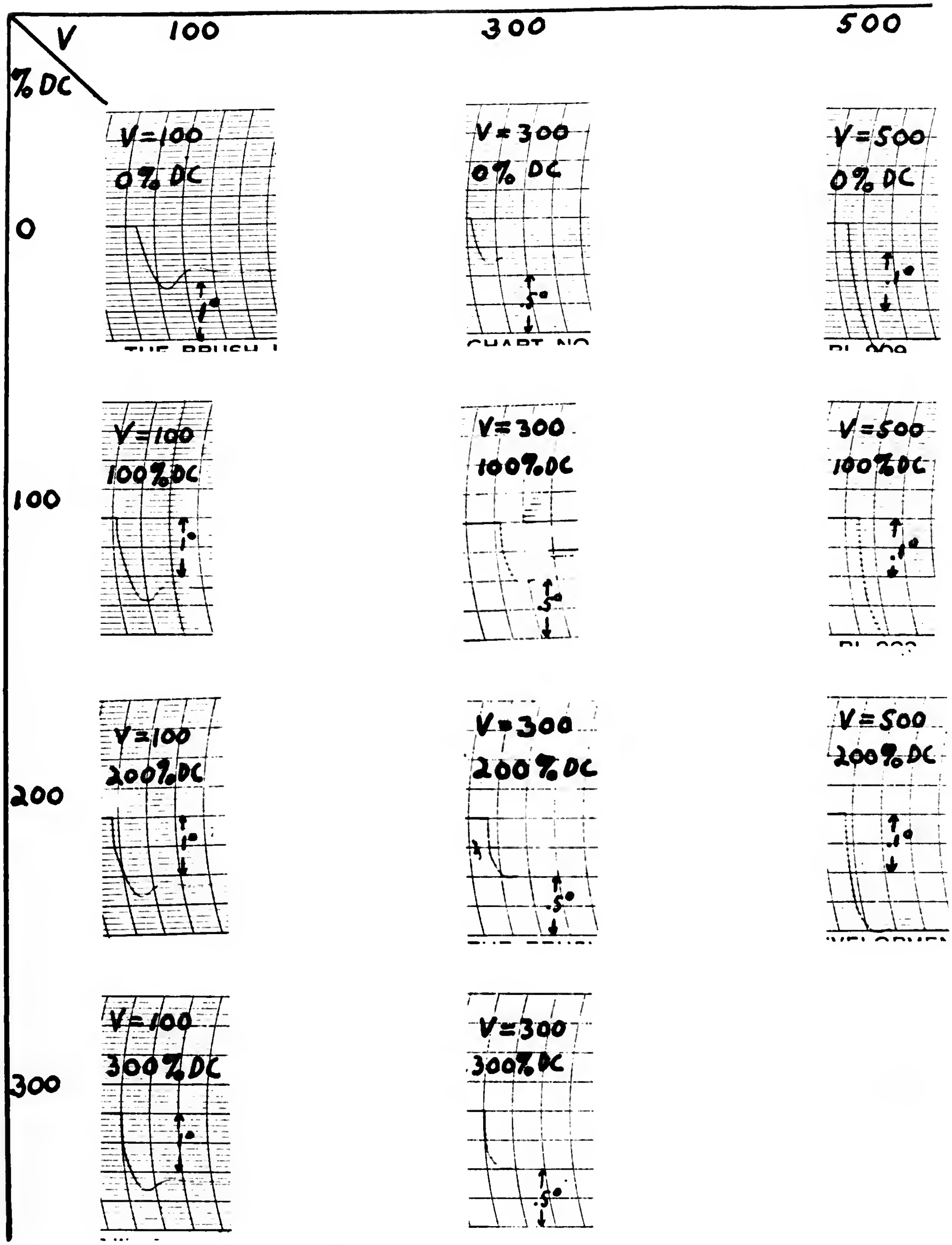

Oscillograph Solutions of Variable $(\beta - \beta^*)$
Step 2.

Figure 23.

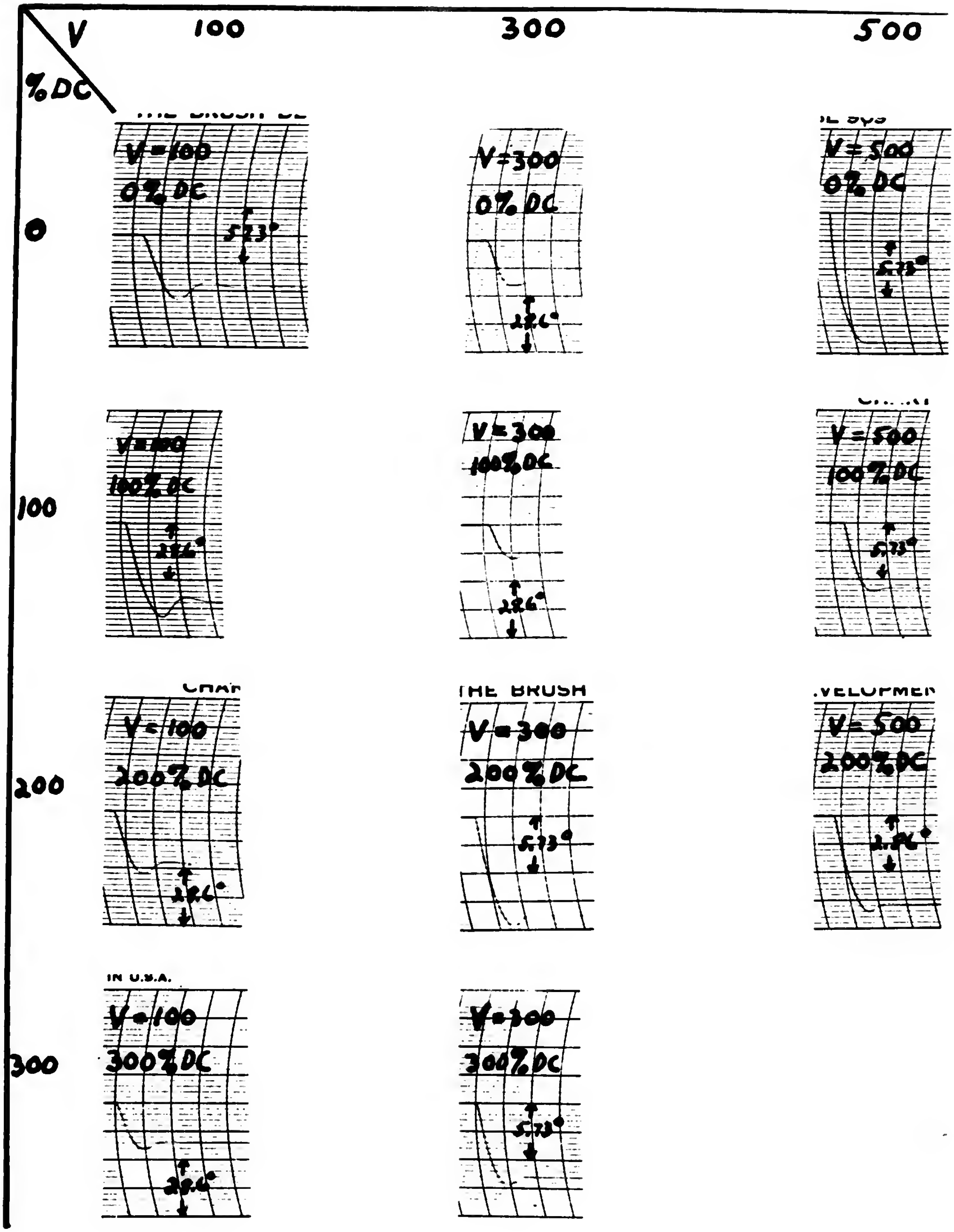

Oscillograph Solutions of Variable (θ).
Step 2.

Figure 24.

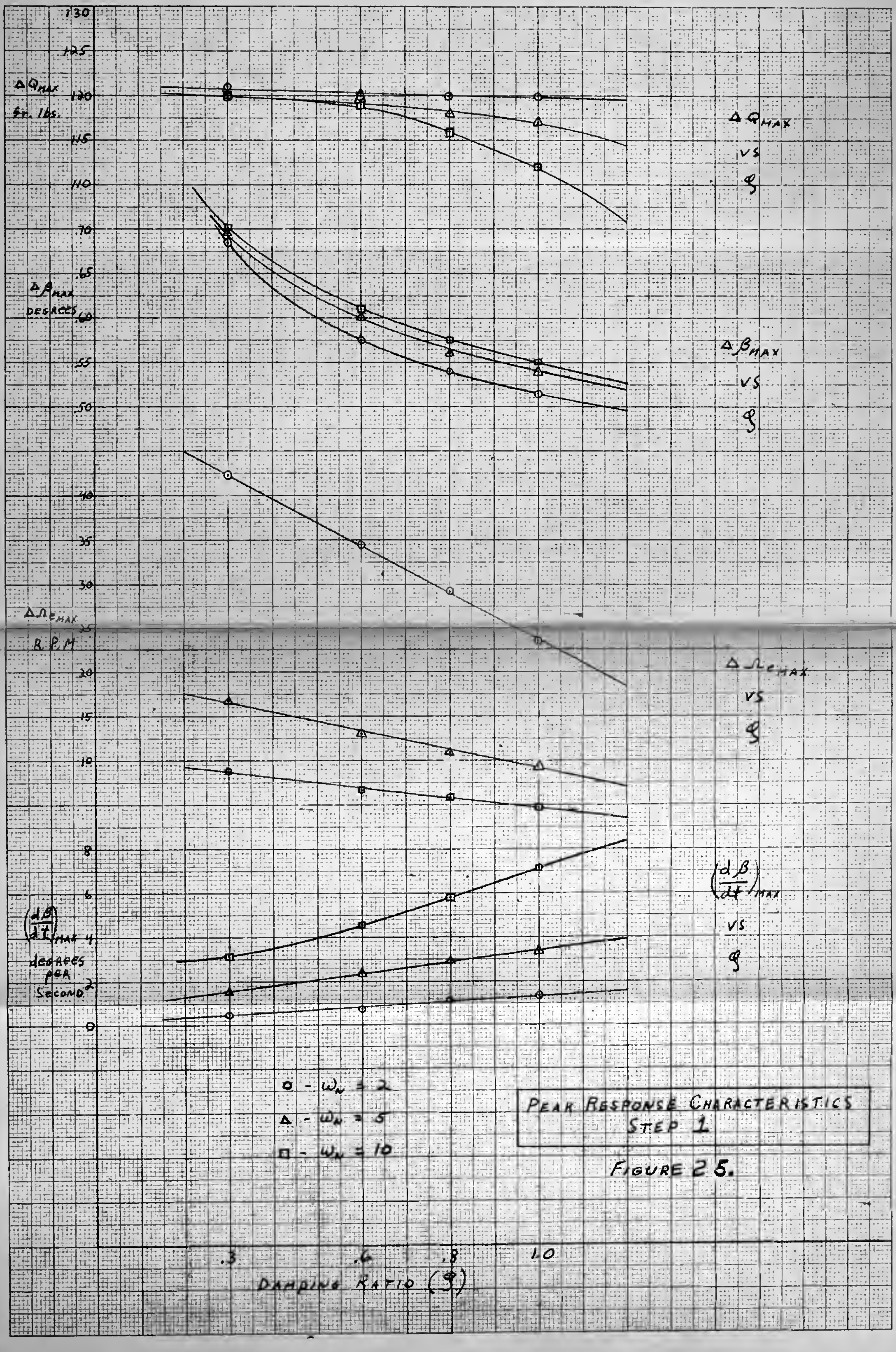

PEAK RESPONSE CHARACTERISTICS
STEP 1

FIGURE 25.

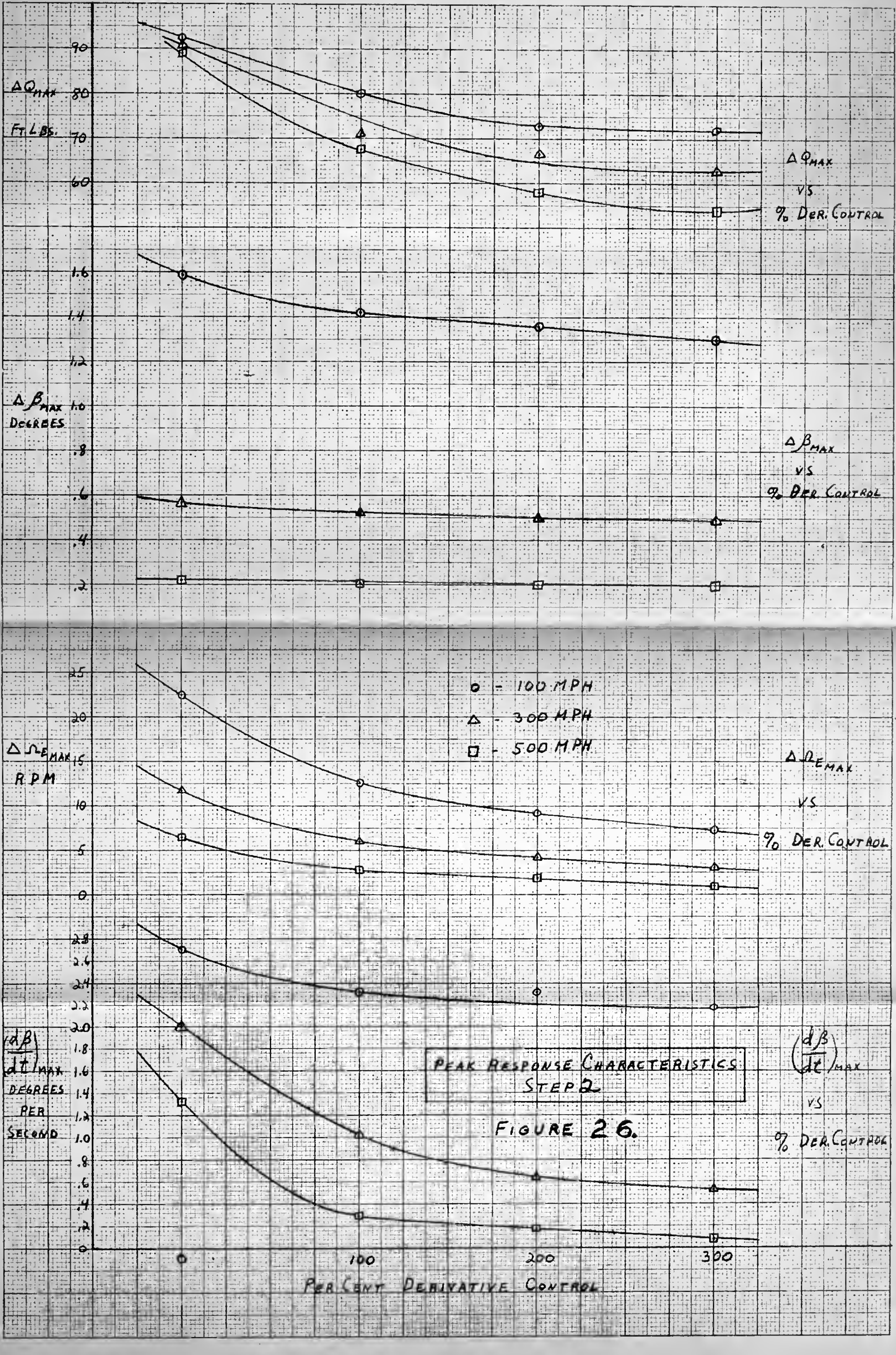

PEAK RESPONSE CHARACTERISTICS
STEP 2

FIGURE 26.

CHANGE IN β $\left(\frac{d\beta}{dt} \rightarrow \infty\right)$

VS

% DERIVATIVE CONTROL

FIGURE 27.

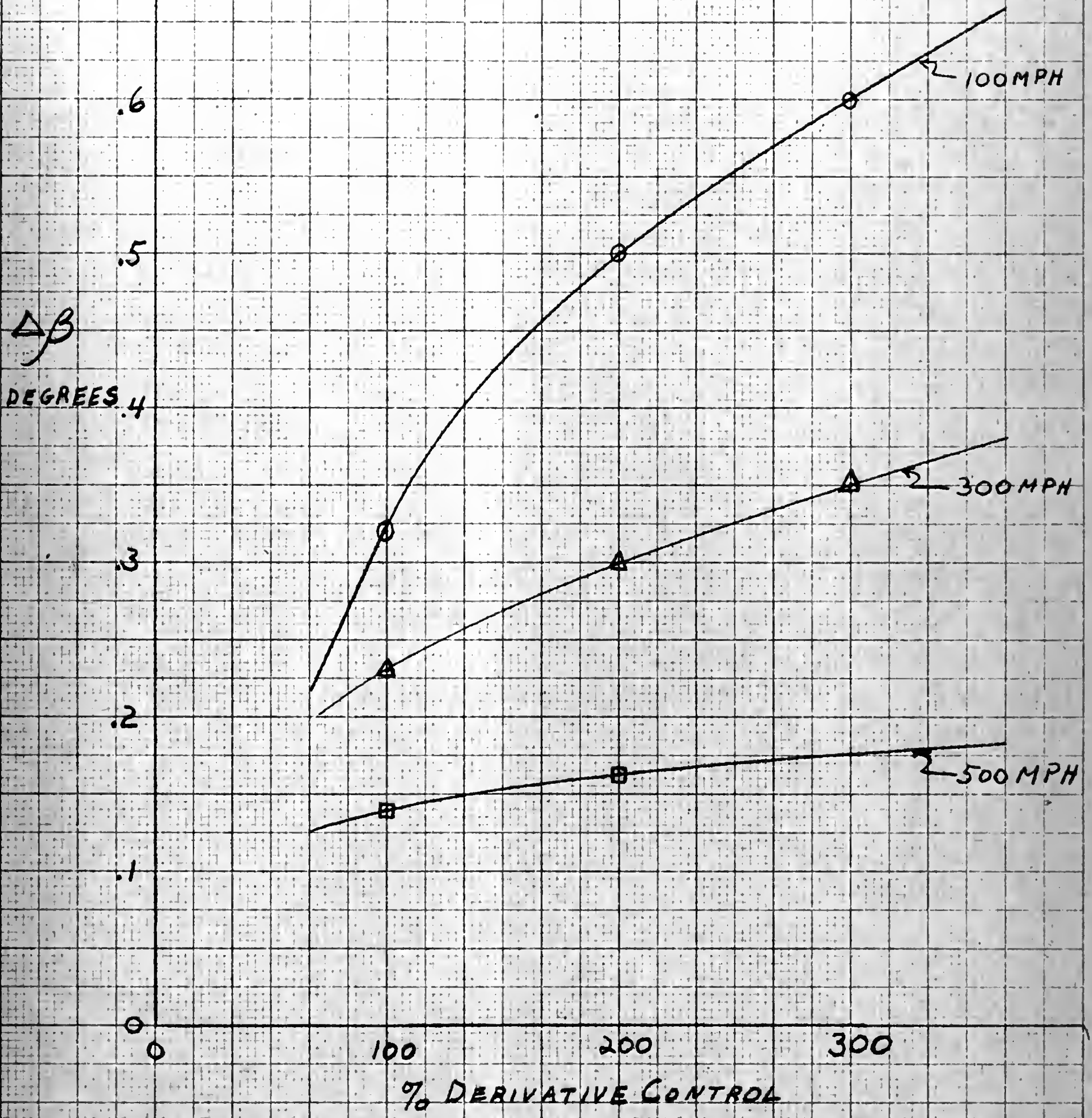

2